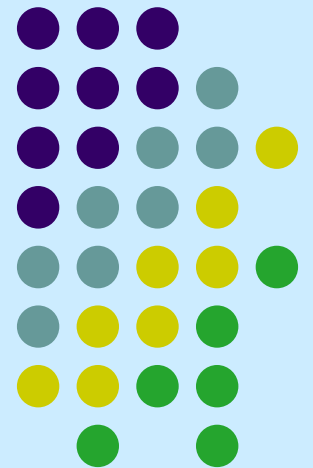
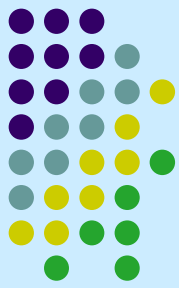


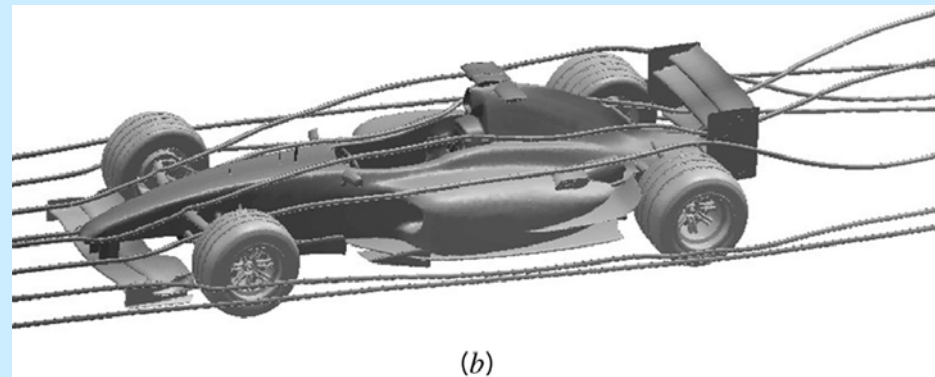
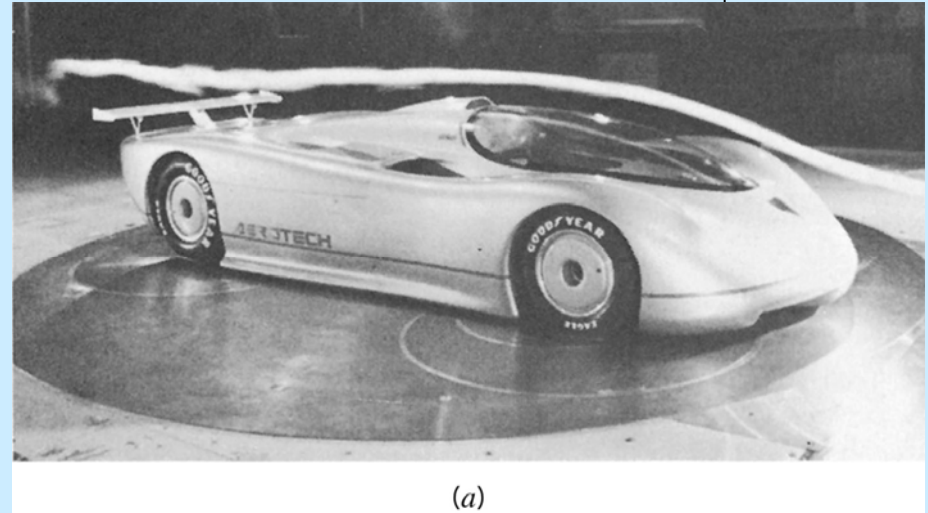
Chapter 9

Flow over Immersed Bodies

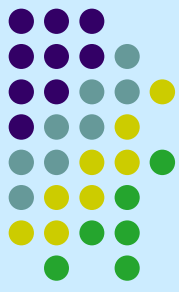




- We consider flows over bodies that are immersed in a fluid and the flows are termed **external flows**.
- We are interested in the fluid force (**lift** and **drag**) over the bodies. For example, **correct design** of cars, trucks, ships, and airplanes, etc. **can greatly decrease the fuel consumption and improve the handling characteristics of the vehicle.**



9.1 General External Flow Characteristics



- A body immersed in a moving fluid experiences a resultant force due to the interaction between the body and the fluid surrounding it.
- Object and flow relation:
stationary air with moving object or
flowing air with stationary object
- Flow classification:

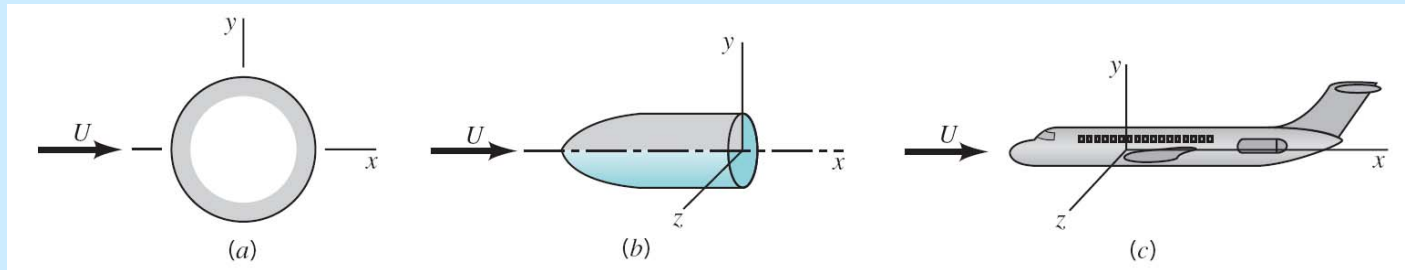
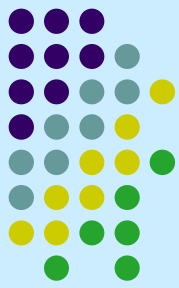


Figure 9.2

Flow classification: (a) two-dimensional, (b) axisymmetric, (c) three-dimensional.

- Body shape:
Streamlined bodies or blunt bodies

9.1.1 Lift and Drag Concepts



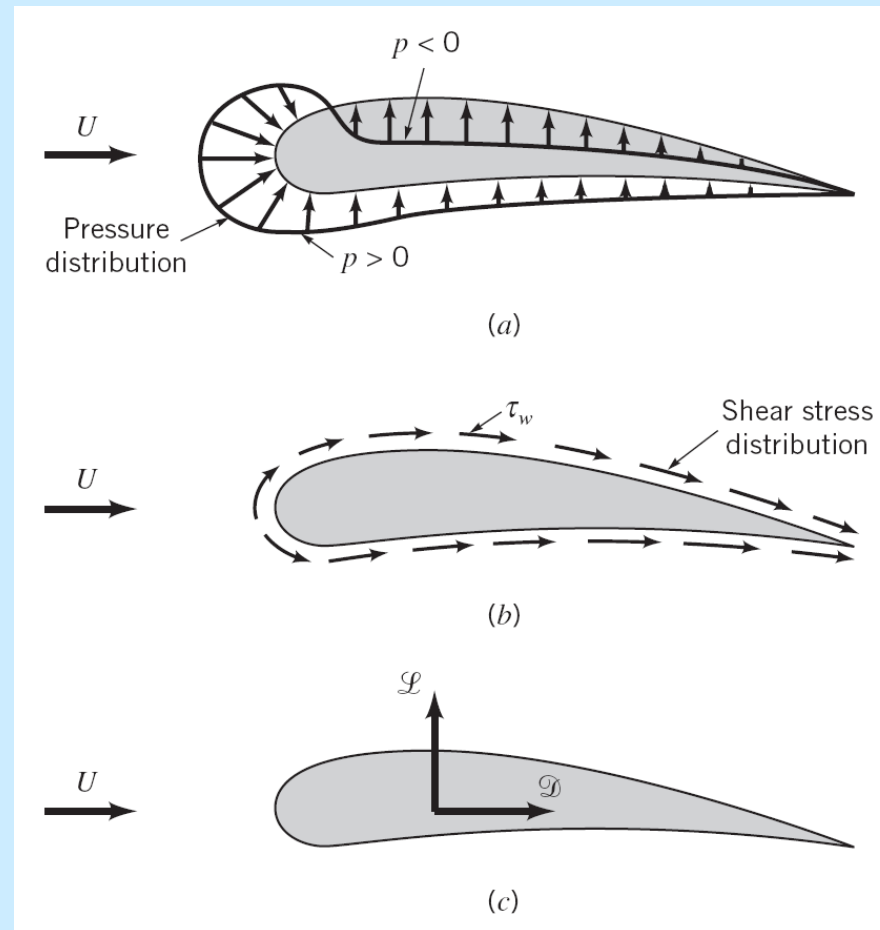
- When any body moves through a fluid, an interaction between the body and the fluid occurs
- This can be described in terms of the stresses-wall shear stresses due to viscous effect and normal stresses due to the pressure P

- **Drag, D**

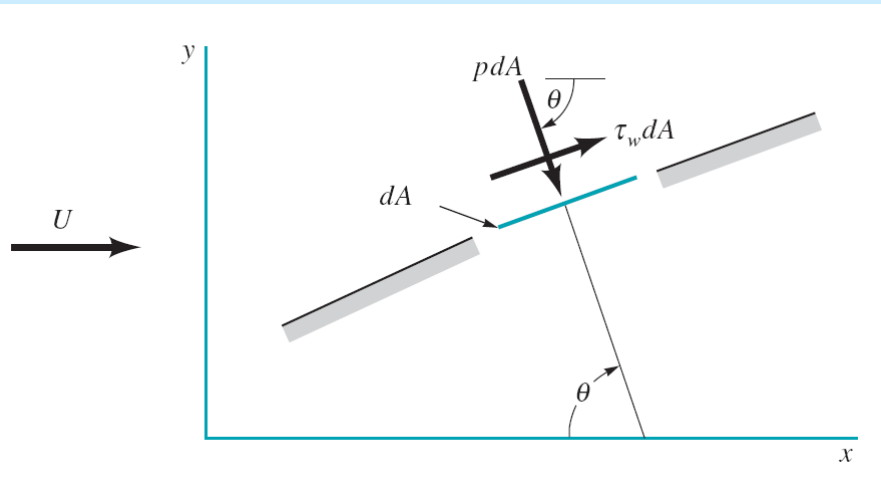
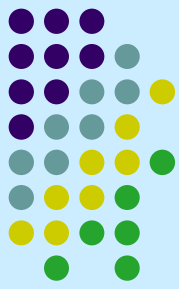
the resultant force in the direction of the upstream velocity

- **Lift, L**

the resultant force normal to the upstream velocity



Resultant force--lift and drag



$$dF_x = (pdA) \cos \theta + (\tau_w dA) \sin \theta$$

and

$$dF_y = -(pdA) \sin \theta + (\tau_w dA) \cos \theta$$

The net x and y components of the force on the object are,

$$D = \int dF_x = \int p \cos \theta dA + \int \tau_w \sin \theta dA$$

$$L = \int dF_y = -\int p \sin \theta dA + \int \tau_w \cos \theta dA$$

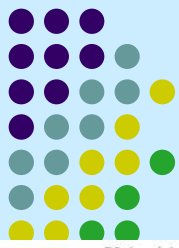
- Nondimensional lift coeff. C_L and drag coeff. C_D

$$C_L = \frac{L}{\frac{1}{2} \rho U^2 A}, \quad C_D = \frac{D}{\frac{1}{2} \rho U^2 A}$$

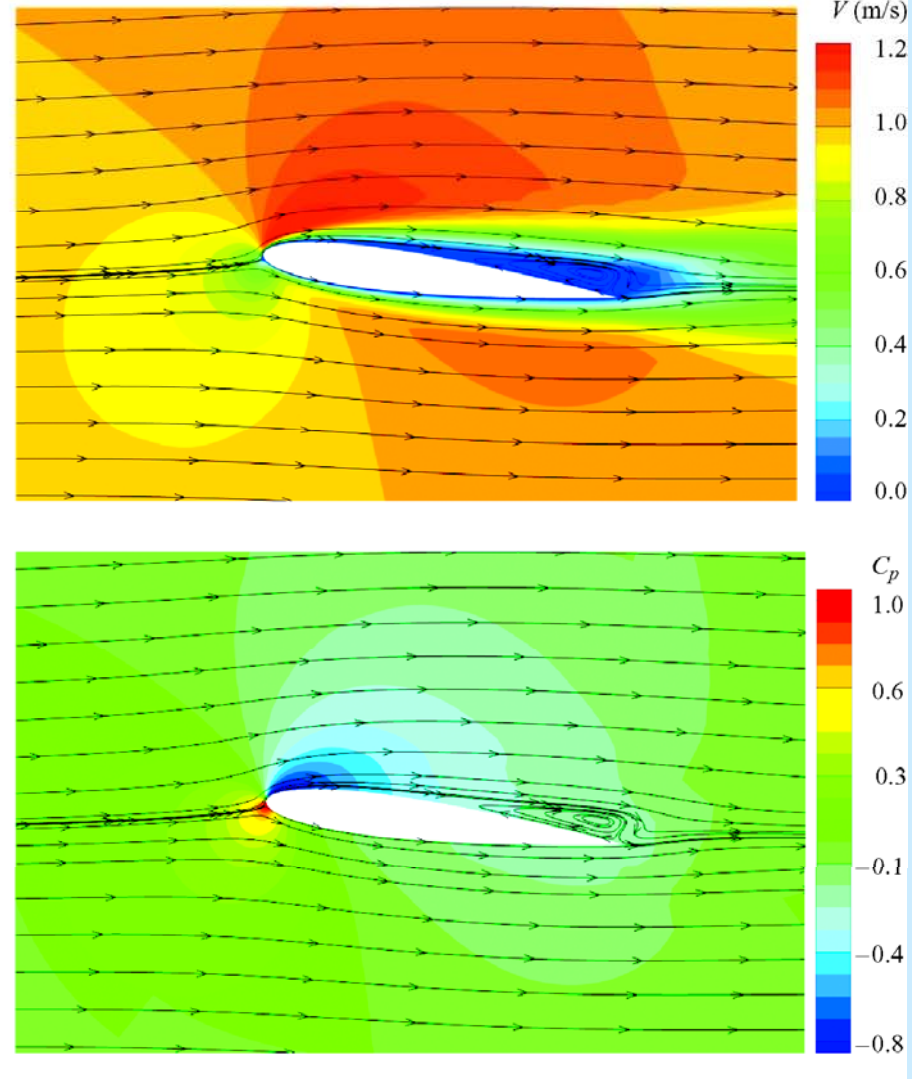
A : characteristic area, frontal area or planform area?

Note: When C_D or $C_L=1$, then D or L equals the dynamic pressure on A .

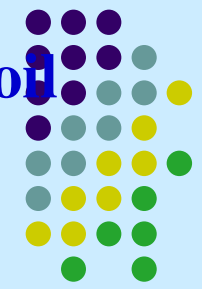
Velocity and pressure distribution around an air foil



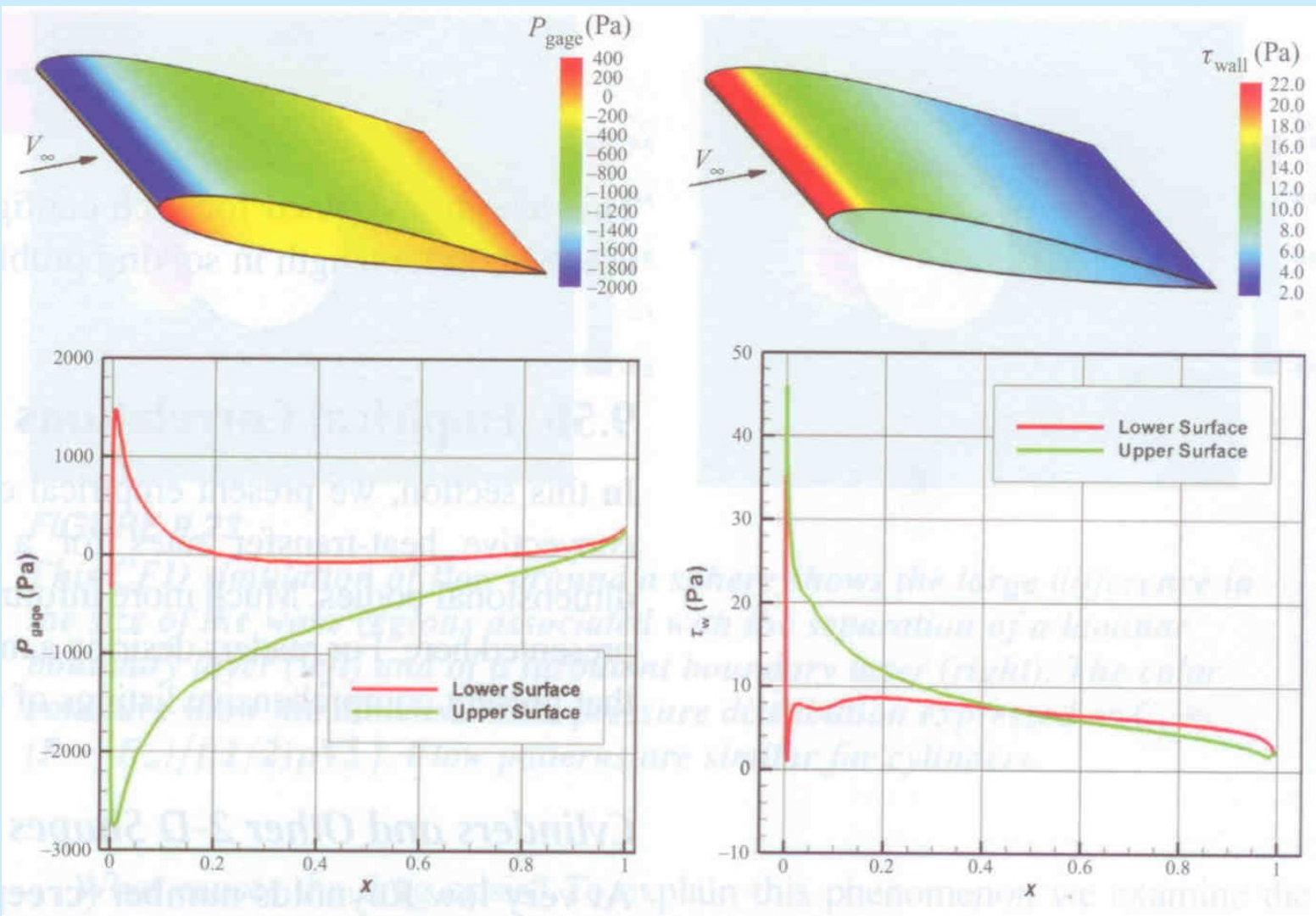
At a 7° angle of attack the boundary layer separates from the upper surface of this airfoil, whereas the boundary layer remains attached to the lower surface. Low velocities (top panel) are evident over much of the upper surface. The corresponding pressure distribution (bottom panel) is expressed using the pressure coefficient C_p . A C_p value of zero corresponds to the ambient pressure, with positive pressure indicated by $C_p > 0$ and negative pressures (vacuum) by $C_p < 0$. From the pressure distribution, we see that very little lift (net upward-directed pressure force) is generated at this condition.



(From S.R. Turns, Thermal-Fluid Sciences, Cambridge Univ. Press, 2006)



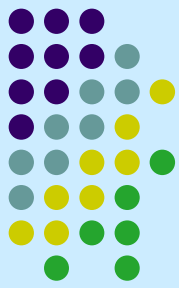
Drag and lift due to *pressure* and *friction*: example of an air foil



CFD results for $Re = 10^6$ show that pressure forces dominate the lift and drag for an airfoil (NACA 0012) at a 5° angle of attack. Here wall shear stresses (right) are about two orders of magnitude less than surface pressures (left).

(From S.R. Turns, Thermal-Fluid Sciences, Cambridge Univ. Press, 2006)

9.1.2 Characteristics of Flow Past an Object



- For typical external flows the most important of parameters are

the **Reynolds number** $Re = \frac{\rho U l}{\mu}$

the **Mach number** $Ma = U/c$

the **Froude number**, for flow with a free surface

$$Fr = \frac{U}{\sqrt{gl}}$$

- Flows with $Re > 100$ are dominated by inertia effects, whereas flows with $Re < 1$ are dominated by viscous effects.

Flow past a flat plate (streamlined body)

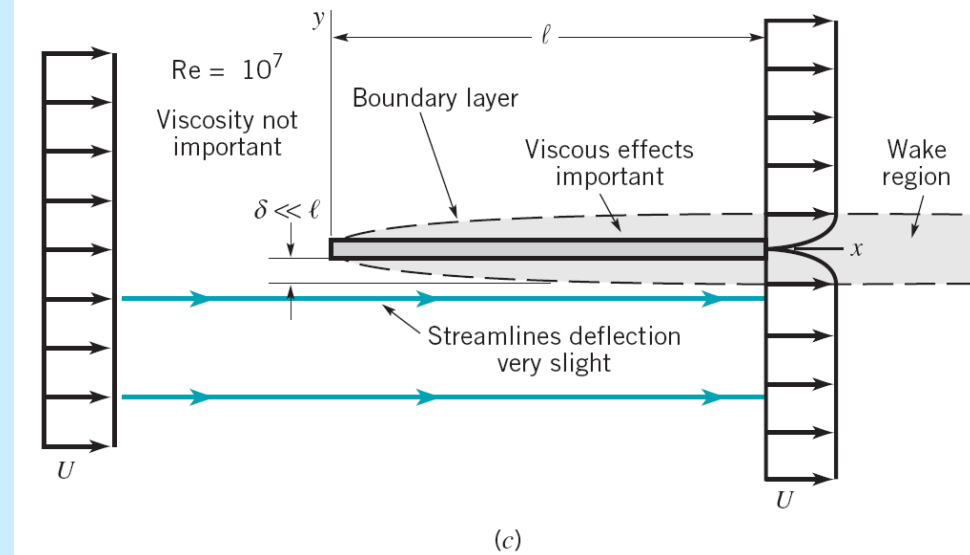
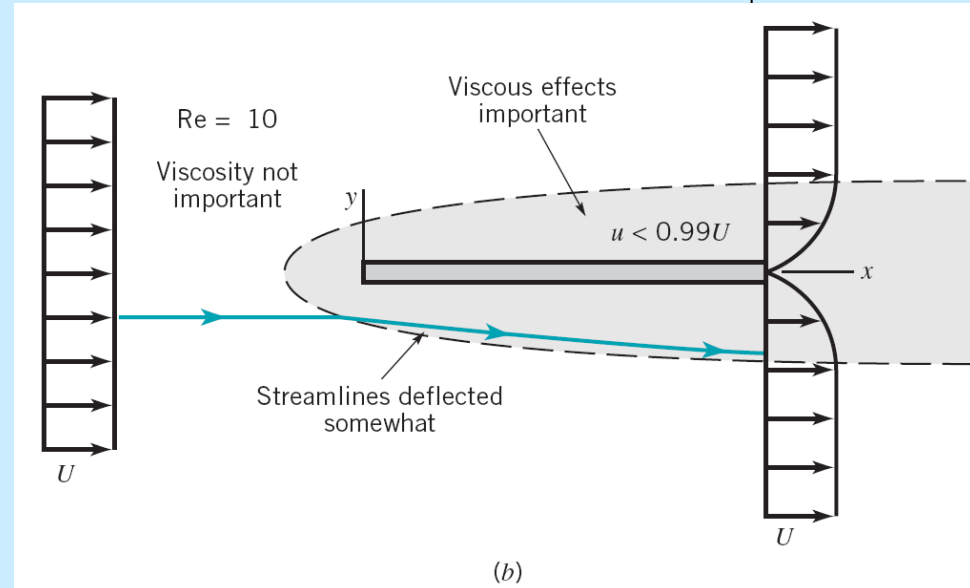
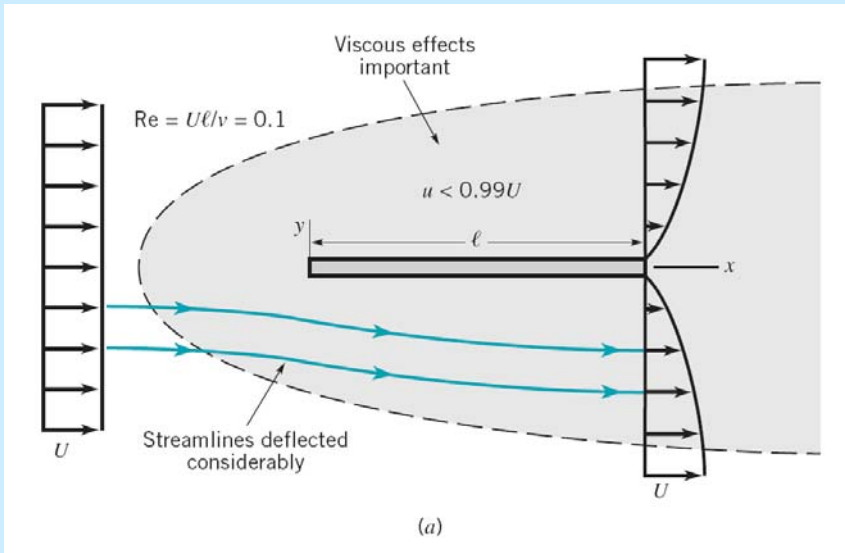
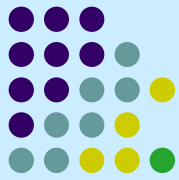
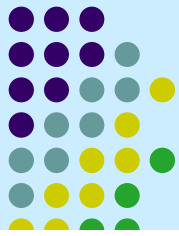
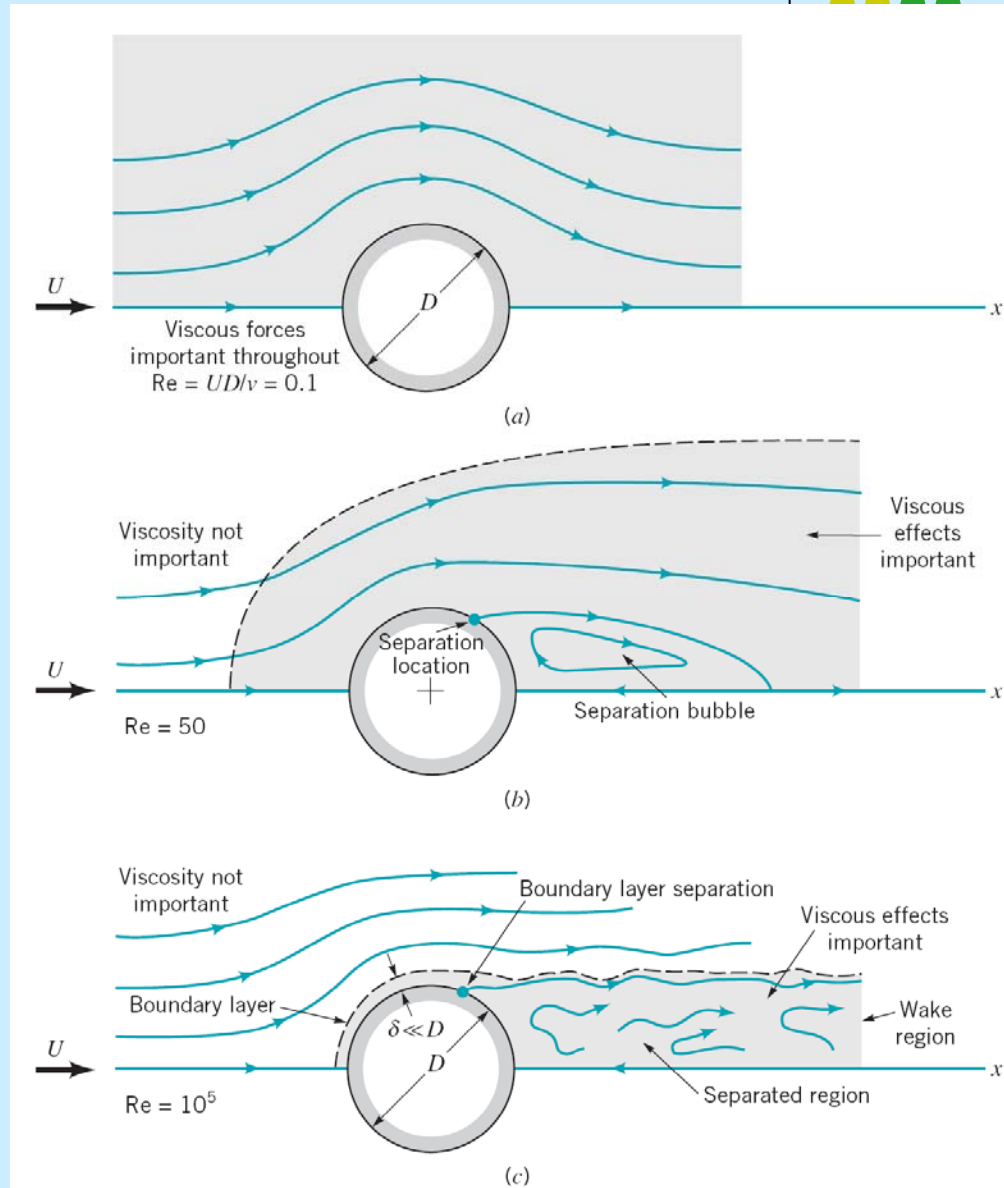


Figure 9.5
Character of the steady, viscous flow past a flat plate parallel to the upstream velocity: (a) low Reynolds number flow, (b) moderate Reynolds number flow, (c) large Reynolds number flow.

Steady flow past a circular cylinder (blunt body)



- The velocity gradients within the boundary layer and wake regions are much larger than those in the remainder of the flow fluid.
- Therefore, viscous effects are confined to the boundary layer and wake regions.



9.2 Boundary Layer Characteristics

9.2.1 Boundary Layer Structure and Thickness on a Flat Plate

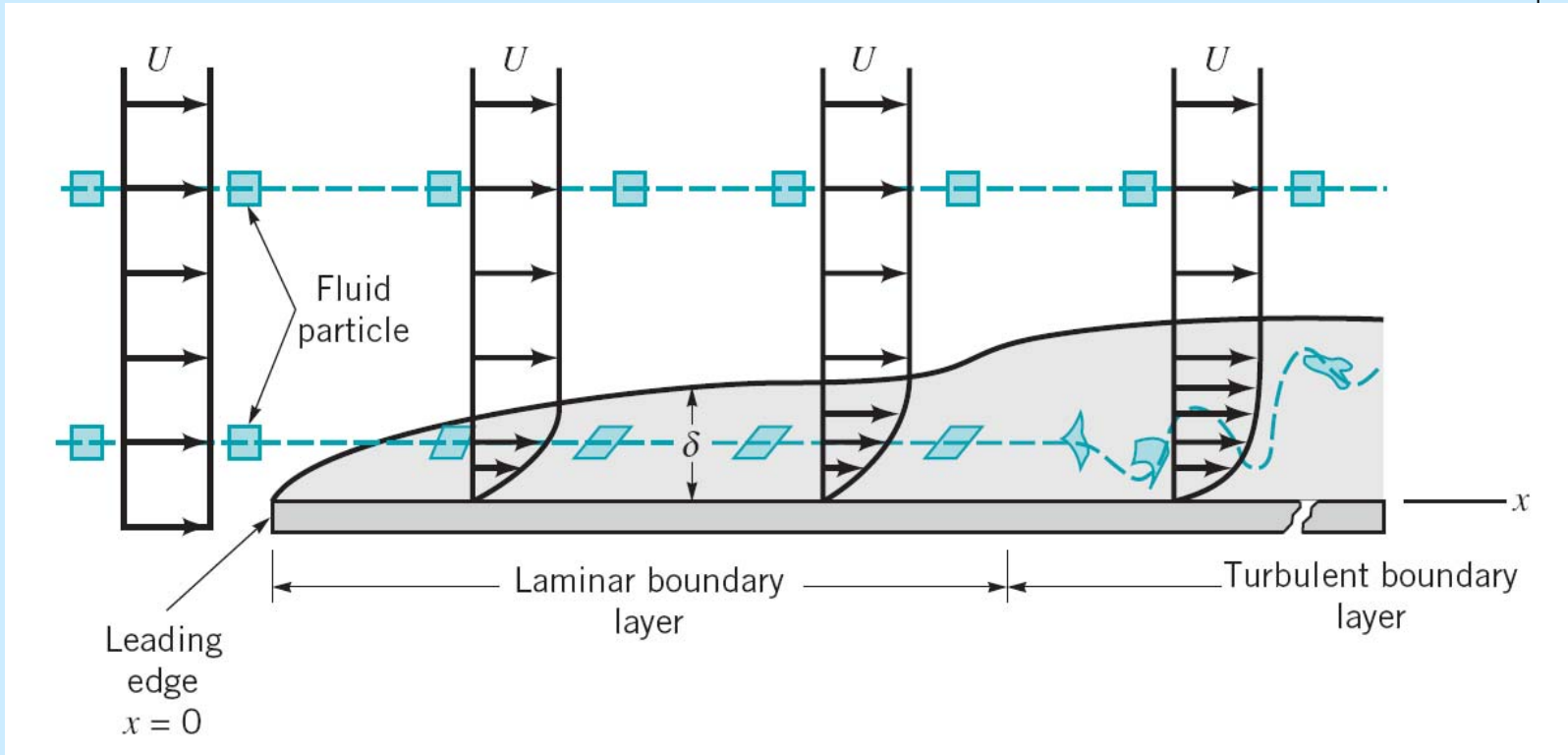
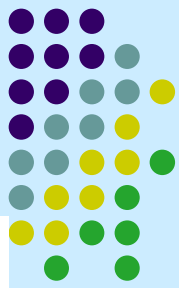


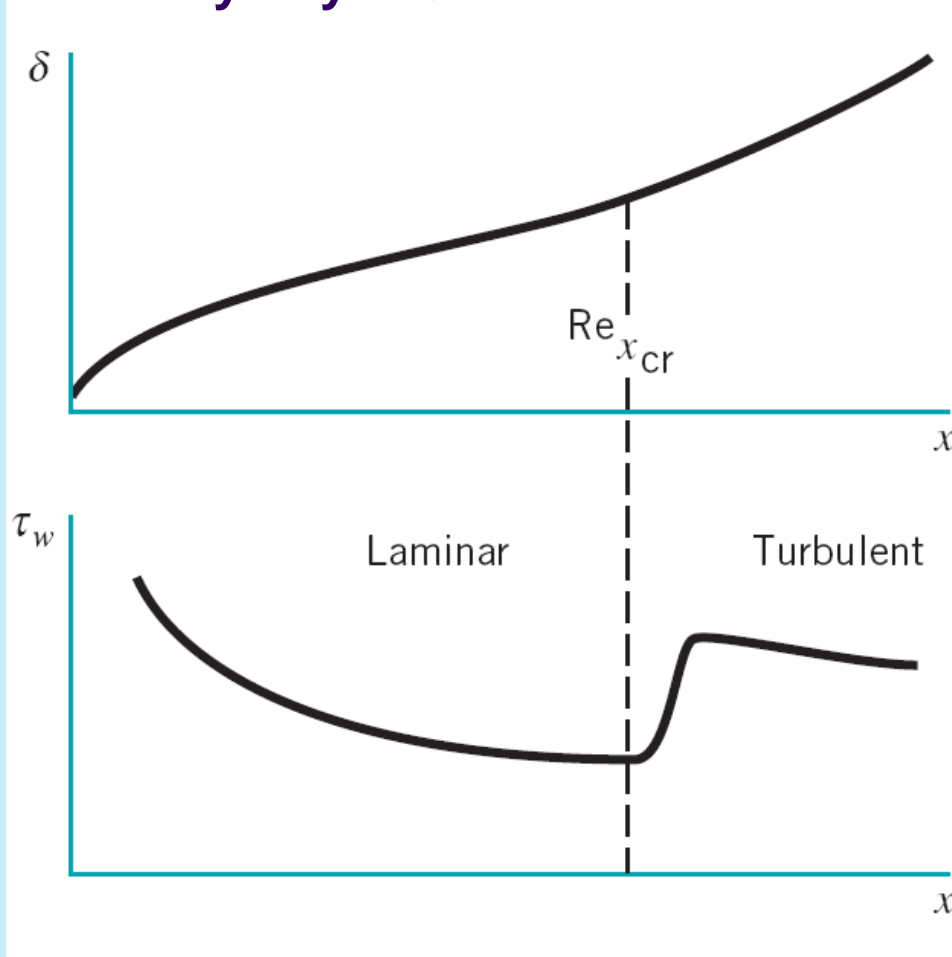
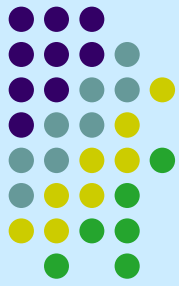
Figure 9.7

Distortion of a fluid particle as it flows within the boundary layer.

- Boundary layer thickness, δ

$$\delta = y \text{ where } u=0.99U$$

Boundary Layer Structure and Thickness on a Flat Plate



Transition occurs at

$$Re_{x_{cr}} = \frac{\rho U x}{\mu} = 2 \times 10^5 \sim 3 \times 10^6$$

depending on surface roughness and amount of turbulence in upstream flow

Figure 9.9

Typical characteristics of boundary layer thickness and wall shear stress for laminar and turbulent boundary layers.

[V9.3 Laminar boundary layer](#)

[V9.4 Laminar/turbulent transition](#)

Boundary layer displacement thickness

$$\delta^* b U = \int_0^{\infty \text{ or } \delta} (U - u) b dy$$

$$\delta^* = \int_0^{\infty} \left(1 - \frac{u}{U} \right) dy$$

(9.3)

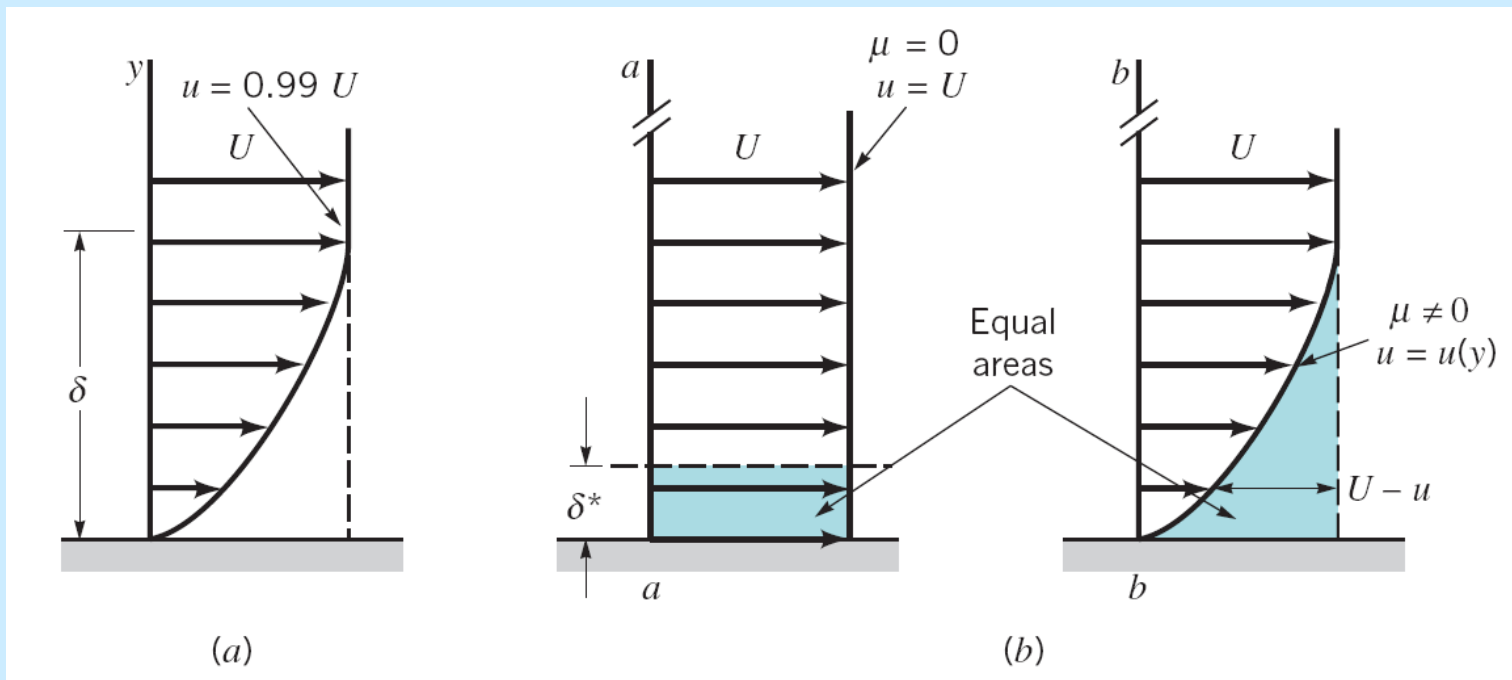
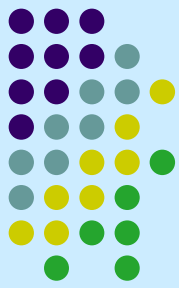


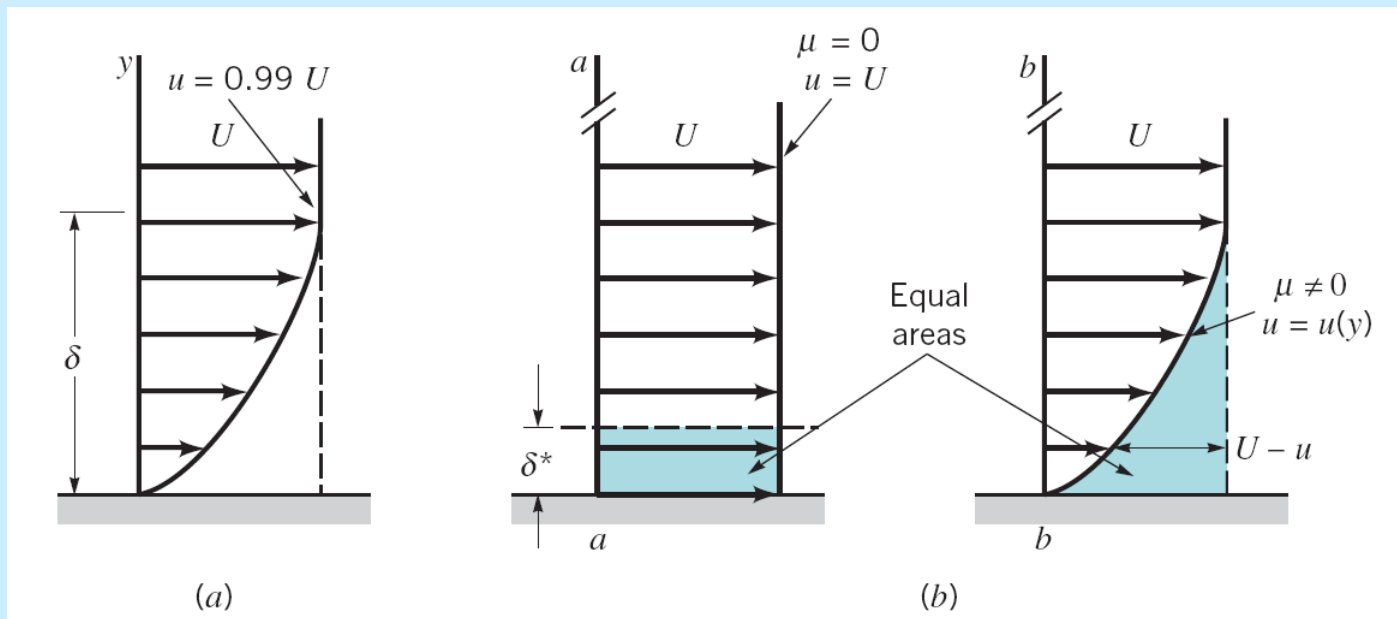
Figure 9.8 (p. 472)

Boundary layer thickness: (a) standard boundary layer thickness, (b) boundary layer displacement thickness.

Boundary layer displacement thickness

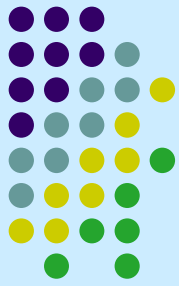


- Represents the amount that the thickness of the body must be increased so that the fictitious uniform inviscid flow has the same mass flow rate properties as the actual viscous flow.
- It represents the outward displacement of the streamlines caused by the viscous effects on the plate.



Ex 9.3 Determine the velocity $U=U(x)$ of the air within the duct but outside of the boundary layer with $\delta^* = 0.004(x)^{1/2}$

Boundary layer momentum thickness

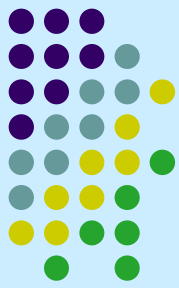


- Boundary layer momentum thickness θ

$$\int \rho u (U - u) dA = \rho b \int_0^{\infty} u (U - u) dy = \rho b U^2 \theta$$

$$\theta = \int_0^{\infty} \frac{u}{U} \left(1 - \frac{u}{U} \right) dy$$

(9.4)



9.2.2 Prandtl/Blasius Boundary Layer Solution

- The Navier-Stokes equations are too complicated that no analytical solution is available. However, for large Re , *simplified boundary layer equations* can be derived.
- 2-D Navier-Stokes Equations

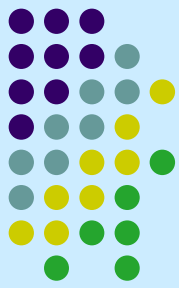
$$u \frac{\partial u}{\partial x} + v \frac{\partial u}{\partial y} = -\frac{1}{\rho} \frac{\partial p}{\partial x} + \nu \left(\frac{\partial^2 u}{\partial x^2} + \frac{\partial^2 u}{\partial y^2} \right) \quad (9.5)$$

$$u \frac{\partial v}{\partial x} + v \frac{\partial v}{\partial y} = -\frac{1}{\rho} \frac{\partial p}{\partial y} + \nu \left(\frac{\partial^2 v}{\partial x^2} + \frac{\partial^2 v}{\partial y^2} \right) \quad (9.6)$$

} Elliptic equation

$$\frac{\partial u}{\partial x} + \frac{\partial v}{\partial y} = 0$$

Boundary layer assumption



- The boundary layer assumption is based on the fact that **the boundary layer is thin**.

$$\delta \ll x \quad \text{so that} \quad v \ll u \quad \text{and} \quad \frac{\partial}{\partial x} \ll \frac{\partial}{\partial y}$$

Thus the equations become,

$$\frac{\partial u}{\partial x} + \frac{\partial v}{\partial y} = 0 \tag{9.8}$$

$$u \frac{\partial u}{\partial x} + v \frac{\partial u}{\partial y} = -\frac{1}{\rho} \frac{\partial p}{\partial x} + \nu \frac{\partial^2 u}{\partial y^2} \tag{9.9}$$

parabolic equation

Detailed derivation is given in Cengel & Cimbala, Fluid Mechanics, 2006, pp. 516-519.

- Physically, the flow is parallel to the plate and any fluid is convected downstream much more quickly than it is diffused across the streamlines.
- For boundary layer flow over a flat plate **the pressure is constant**. The flow represents a balance between viscous and inertial effects, with pressure playing no role.

Boundary conditions



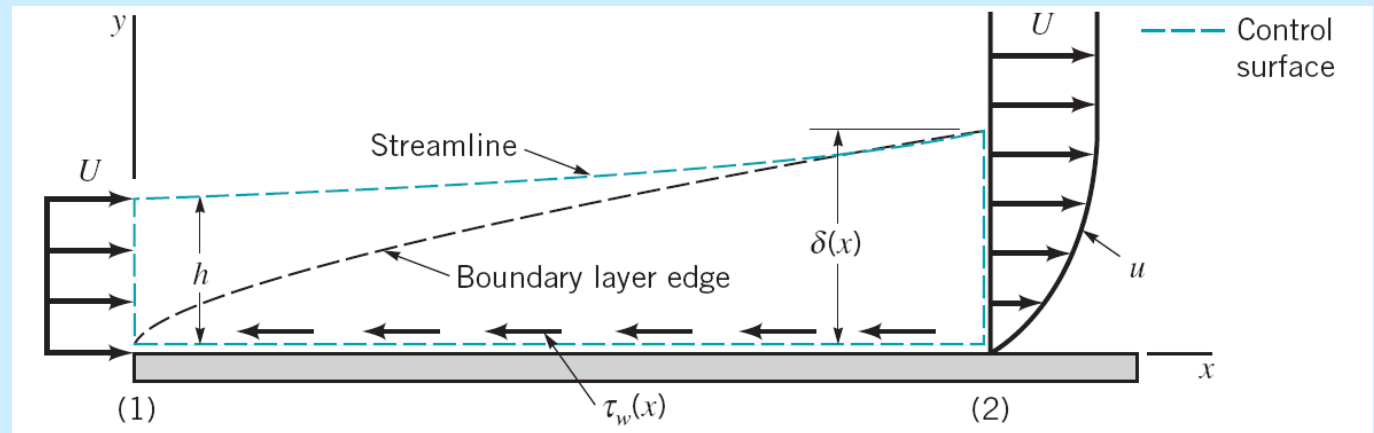
$$\text{BCs: } u = v = 0, \quad y = 0$$
$$u \rightarrow U, \quad y \rightarrow \infty$$

It can be argued that the velocity profile should be similar $\rightarrow \frac{u}{U} = g\left(\frac{y}{\delta}\right)$

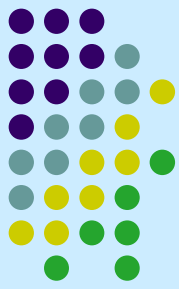
In addition, order of magnitude analysis leads to:

$$u \frac{\partial u}{\partial x} + v \frac{\partial u}{\partial y} = \nu \frac{\partial^2 u}{\partial y^2}, \quad \frac{uu}{x} \sim \frac{\nu u}{\delta^2},$$

$$\delta^2 \sim \frac{\nu x}{U}, \quad \delta \sim \left(\frac{\nu x}{U}\right)^{1/2}$$



Similarity variables



Define the dimensionless similarity variable

$$\eta = \left(\frac{U}{\nu x} \right)^{1/2} y \sim \frac{y}{\delta},$$

and stream function

$$\psi = (\nu x U)^{1/2} f(\eta) \quad \text{where } f(\eta) \text{ is an unknown function}$$

Thus

$$\begin{cases} u = \frac{\partial \psi}{\partial y} = (\nu x U)^{1/2} f'(\eta) \left(\frac{U}{\nu x} \right)^{1/2} = U f'(\eta) \\ v = -\frac{\partial \psi}{\partial x} = \left(\frac{\nu U}{4x} \right)^{1/2} (\eta f' - f) \quad \text{where } ()' = d/d\eta \end{cases}$$

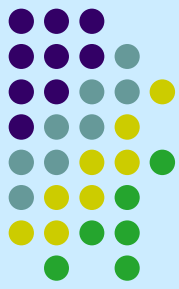
Then the parabolic equation (9.9) becomes

$$2f''' + ff'' = 0 \tag{9.14a}$$

with the boundary conditions

$$f(0) = f'(0) = 0 \quad \text{at } \eta = 0, \quad f'(\infty) \rightarrow 1 \quad \text{as } \eta \rightarrow \infty \tag{9.14b}$$

Blasius solutions



$$\frac{u}{U} = f'(\eta)$$

from the numerical solution $\frac{u}{U} \approx 0.99 \quad \eta = 5.0$ (Table 9.1)

$$\eta = 5 = \left(\frac{U}{\nu x}\right)^{1/2} \delta, \quad \delta = 5\sqrt{\frac{\nu x}{U}}$$

or $\frac{\delta}{x} = \frac{5}{\sqrt{\text{Re}_x}} \quad \sqrt{\text{Re}_x} = \frac{Ux}{\nu}$

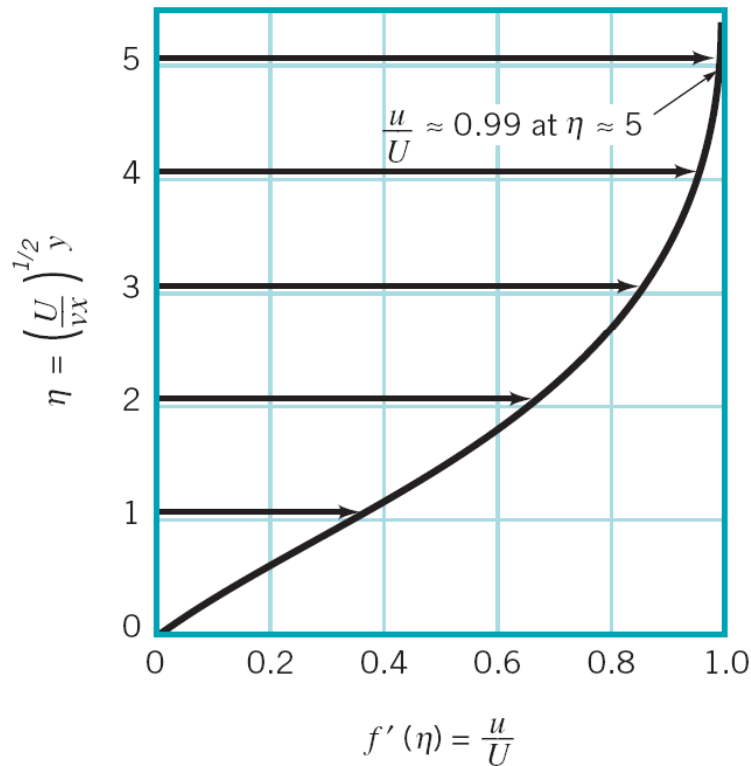
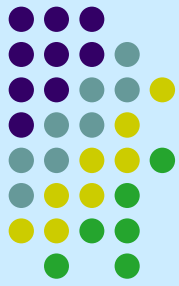
HW: Derive (9.14&9.18) and solve using Matlab to get Table 9.1

■ TABLE 9.1

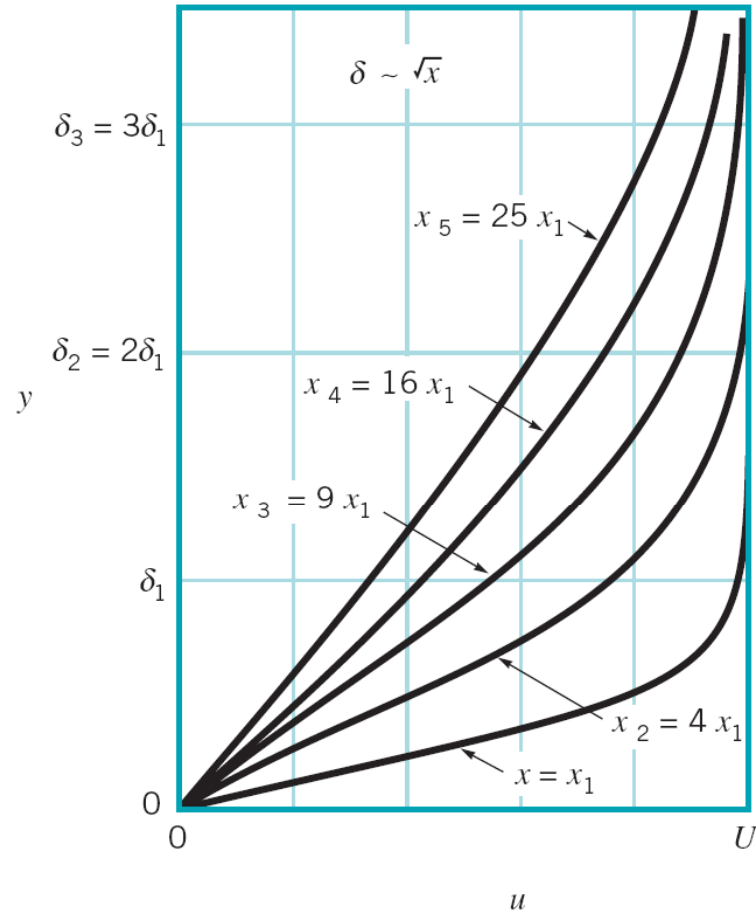
Laminar Flow along a Flat Plate
(the Blasius Solution)

$\eta = y(U/\nu x)^{1/2}$	$f'(\eta) = u/U$	η	$f'(\eta)$
0	0	3.6	0.9233
0.4	0.1328	4.0	0.9555
0.8	0.2647	4.4	0.9759
1.2	0.3938	4.8	0.9878
1.6	0.5168	<u>5.0</u>	<u>0.9916</u>
2.0	0.6298	5.2	0.9943
2.4	0.7290	5.6	0.9975
2.8	0.8115	6.0	0.9990
3.2	0.8761	∞	1.0000

Blasius solution



(a)



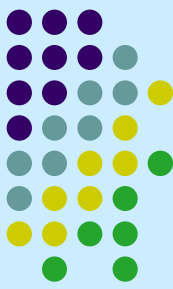
(b)

Figure 9.10

Blasius boundary layer profile: (a) boundary layer profile in dimensionless form using the similarity variable η . (b) similar boundary layer profiles at different locations along the flat plate.

Blasius solution

displacement thickness: from (9.3) $\rightarrow \frac{\delta^*}{x} = \frac{1.721}{\sqrt{\text{Re}_x}}$



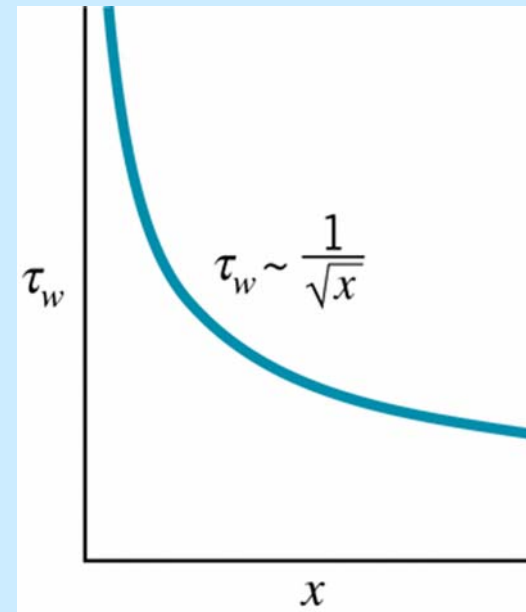
(9.16)

momentum thickness: from (9.4) $\rightarrow \frac{\theta}{x} = \frac{0.664}{\sqrt{\text{Re}_x}}$

(9.17)

boundary layer Shear stress:

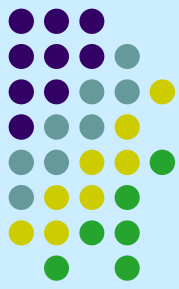
$$\tau_w = \mu \left. \frac{\partial u}{\partial y} \right|_{y=0} = 0.332U^{3/2} \sqrt{\frac{\rho\mu}{x}}$$



(9.18)

Note: For fully developed pipe flow shear stress, $\tau_w \propto U$ (why?)

9.2.3 Momentum-Integral Boundary Layer Equation for a Flat Plate



- One of the important aspects of boundary layer theory is the determination of the **drag** caused by shear forces on a body.
- Consider a uniform flow past a flat plate

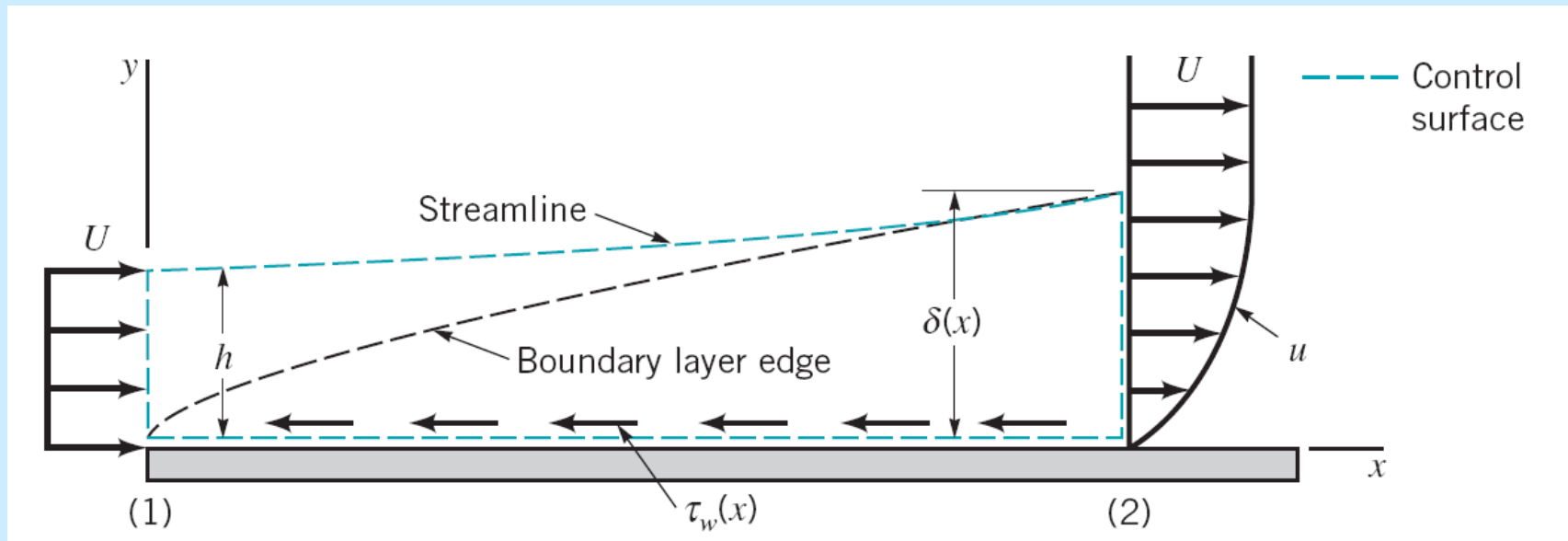


Figure 9.11

Control volume used in the derivation of the momentum integral equation for boundary layer flow.

x-component of momentum equation:

$$\sum F_x = \rho \int_{(1)} u \bar{V} \bar{n} dA + \rho \int_{(2)} u \bar{V} \bar{n} dA$$

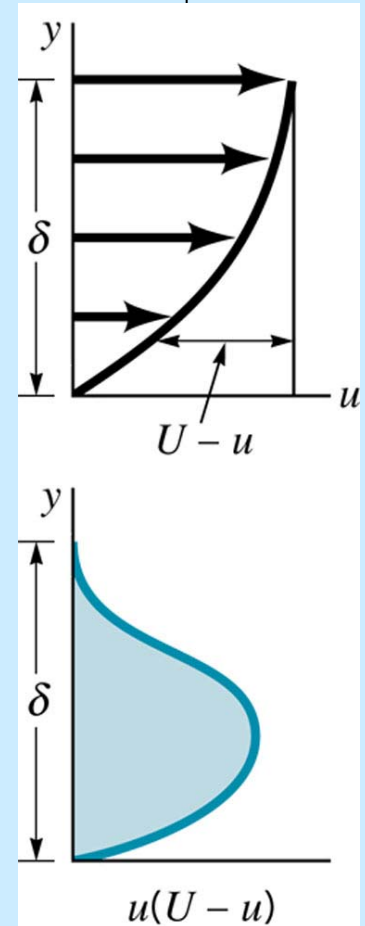
$$\sum F_x = -D = - \int_{plate} \tau_w dA = -b \int_{plate} \tau_w dx \quad \text{or}$$

$$-D = \rho \int_{(1)} U(-U) dA + \rho \int_{(2)} u^2 dA \quad \rightarrow \quad D = \rho U^2 bh - \rho b \int_0^\delta u^2 dy$$

$$\text{Since } Uh = \int_0^\delta u dy, \quad \rho U^2 bh = \rho b U \int_0^\delta u dy = \rho b \int_0^\delta U u dy$$

$$D = \rho U^2 bh - \rho b \int_0^\delta u^2 dy = \rho b \int_0^\delta U u dy - \rho b \int_0^\delta u^2 dy = \rho b \int_0^\delta u(U - u) dy$$

$$D = \rho b U^2 \int_0^\delta \frac{u}{U} \left(1 - \frac{u}{U}\right) dy = \rho b U^2 \theta, \quad \text{and} \quad \frac{dD}{dx} = \rho b U^2 \frac{d\theta}{dx}$$



The increase in drag per length of the plate occurs at the expense of an increase of the momentum boundary layer thickness, which represents a decrease in the momentum of the fluid.

$$\therefore dD = \tau_w b dx \rightarrow \frac{dD}{dx} = b \tau_w \quad \therefore \tau_w = \rho U^2 \frac{d\theta}{dx} \rightarrow \text{momentum integral equation by von Karman}$$

Momentum integral equation

$$\tau_w = \rho U^2 \frac{d\theta}{dx} \rightarrow \text{momentum integral equation}$$

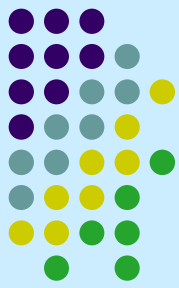
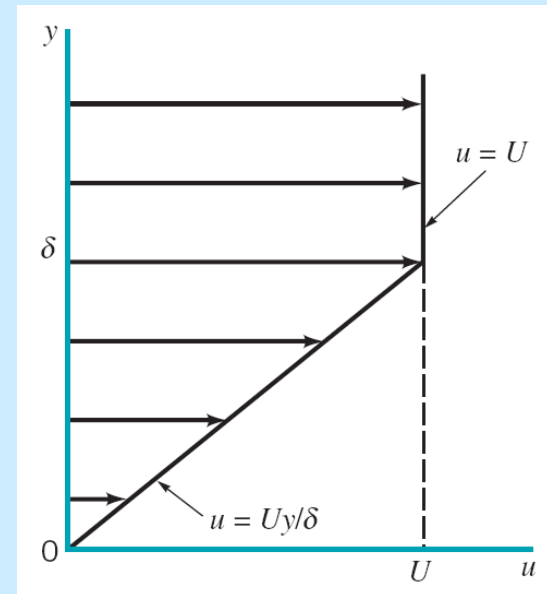
- If we know the velocity distributions, we can obtain drag or shear stress.
- The accuracy of these results depends on how closely the shape of the assumed velocity profile approximates the actual profile.

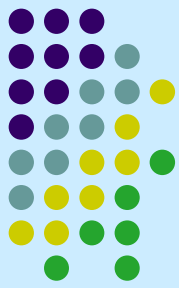
Example 9.4

$$u = \frac{Uy}{\delta} \quad 0 \leq y \leq \delta \quad u = U \quad y > \delta$$

$$\tau_w = \rho U^2 \frac{d\theta}{dx}$$

$$\tau_w = \mu \frac{U}{\delta}$$





$$\theta = \int_0^{\infty} \frac{u}{U} \left(1 - \frac{u}{U}\right) dy = \int_0^{\delta} \frac{u}{U} \left(1 - \frac{u}{U}\right) dy$$

$$= \int_0^{\delta} \frac{y}{\delta} \left(1 - \frac{y}{\delta}\right) dy = \delta \int_0^1 (y - y^2) dy = \delta \left(\frac{y^2}{2} - \frac{y^3}{3} \right) \Big|_0^1 = \frac{\delta}{6}$$

$$\frac{\mu U}{\delta} = \frac{\rho U^2}{6} \frac{d\delta}{dx}, \quad \delta d\delta = \frac{6\mu}{\rho U} dx$$

$$\frac{\delta^2}{2} = \frac{6\mu}{\rho U} x \Rightarrow \delta^2 = \frac{12\mu}{\rho U} x$$

or $\delta = 3.46 \sqrt{\frac{\mu x}{\rho U}} \Leftrightarrow$ compare with Blasius solution $\frac{\delta}{x} = 5 \sqrt{\frac{\mu}{\rho U x}}$

$$\frac{\delta}{x} = 3.46 \sqrt{\frac{\mu}{\rho U x}}$$

$$\theta = \frac{\delta}{6} = 0.576 \sqrt{\frac{\mu x}{\rho U}}$$

$$\tau_w = \rho U^2 \frac{d\theta}{dx} = 0.289 U^{3/2} \sqrt{\frac{\rho \mu}{x}} \Leftrightarrow \tau_w = 0.332 U^{3/2} \sqrt{\frac{\rho \mu}{x}}$$

■ **TABLE 9.2**

Flat Plate Momentum Integral Results for Various Assumed Laminar Flow Velocity Profiles

Profile Character	$\delta \text{Re}_x^{1/2} / x$	$c_f \text{Re}_x^{1/2}$	$C_{Df} \text{Re}_l^{1/2}$
a. Blasius solution	5.00	0.664	1.328
b. Linear $u/U = y/\delta$	3.46	0.578	1.156
c. Parabolic $u/U = 2y/\delta - (y/\delta)^2$	5.48	0.730	1.460
d. Cubic $u/U = 3(y/\delta)/2 - (y/\delta)^3/2$	4.64	0.646	1.292
e. Sine wave $u/U = \sin[\pi(y/\delta)/2]$	4.79	0.655	1.310

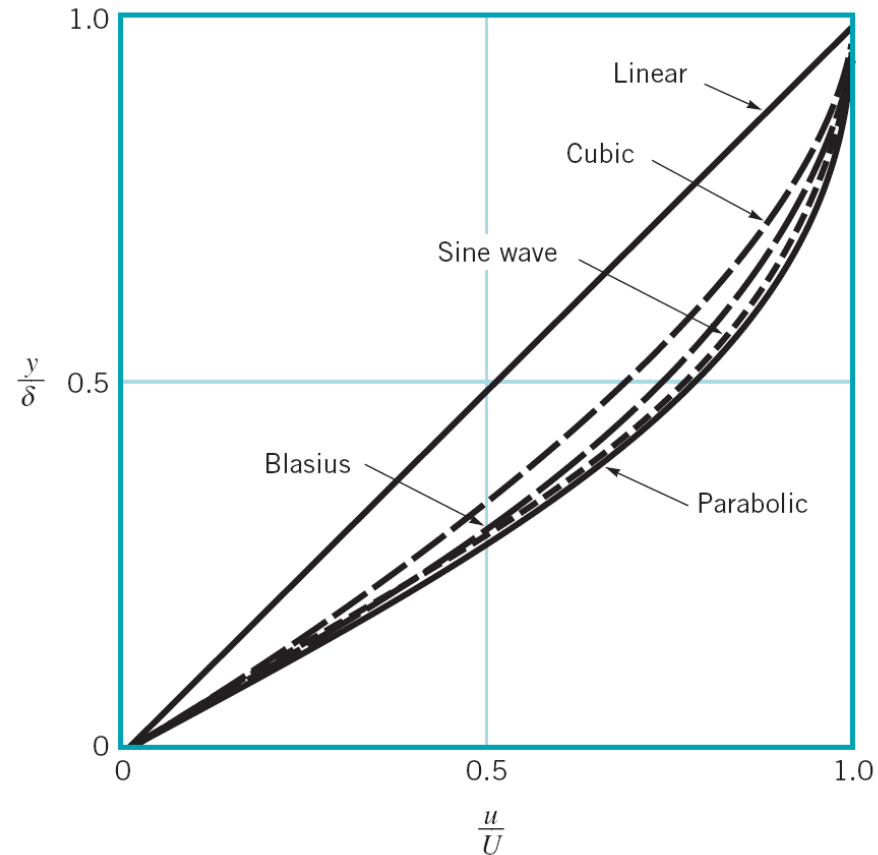
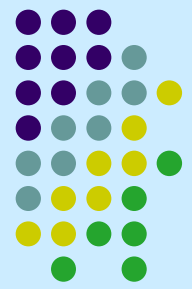
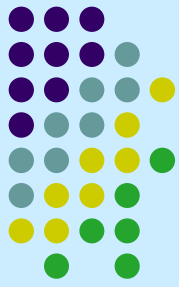


Figure 9.12
Typical approximate boundary layer profiles used in the momentum integral equation.

Momentum integral equation for general profile of u/U



Let $\frac{u}{U} = g(Y)$ for $0 \leq Y \leq 1$, $\frac{u}{U} = 1$ for $Y > 1$, where $Y = \frac{y}{\delta}$

B.C.: $g(0) = 0$, $g(1) = 1$

$$D = \rho b U^2 \int_0^{\delta} \frac{u}{U} \left(1 - \frac{u}{U}\right) dy = \rho b U^2 \delta \int_0^1 g(Y)[1 - g(Y)] dY = \rho b U^2 \delta C_1$$

$$\tau_w = \mu \left. \frac{\partial u}{\partial y} \right|_{y=0} = \frac{\mu U}{\delta} \left. \frac{dg}{dY} \right|_{Y=0} = \frac{\mu U}{\delta} C_2$$

we can obtain that

$$C_1 = \int_0^1 g(Y)[1 - g(Y)] dY$$

$$C_2 = \left. \frac{dg}{dY} \right|_{Y=0}$$

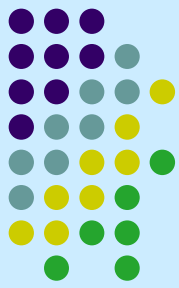
$$\frac{\delta}{x} = \frac{\sqrt{2C_2/C_1}}{\sqrt{\text{Re}_x}} \quad (\text{Blasius solution: } \frac{\delta}{x} = \frac{5}{\sqrt{\text{Re}_x}})$$

$$\tau_w = \frac{\mu U}{\delta} C_2 = \sqrt{\frac{C_1 C_2}{2}} U^{3/2} \sqrt{\frac{\rho \mu}{x}}$$

$$c_f = \frac{\tau_w}{\frac{1}{2} \rho U^2} = \sqrt{2C_1 C_2} \sqrt{\frac{\mu}{\rho U x}} = \frac{\sqrt{2C_1 C_2}}{\sqrt{\text{Re}_x}} \quad (\text{Blasius solution: } c_f = \frac{0.664}{\sqrt{\text{Re}_x}})$$

$$C_{Df} = \frac{D_f}{\frac{1}{2} \rho U^2 b \ell} = \frac{b \int_0^{\ell} \tau_w dx}{\frac{1}{2} \rho U^2 b \ell} = \frac{\sqrt{8C_1 C_2}}{\sqrt{\text{Re}_\ell}}, \quad \text{where } \text{Re}_\ell = \frac{\rho U \ell}{\mu} \quad (\text{Blasius solution: } C_{Df} = \frac{1.328}{\sqrt{\text{Re}_\ell}})$$

9.2.4 Transition from Laminar to Turbulent Flow



- The analytical results are restricted to laminar boundary layer along a flat plate with zero pressure gradient.
- Transition to turbulent boundary layer occurs at

$$Re_{x,cr} = 2 \times 10^5 \square 3 \times 10^6$$

Example 9.5 Boundary layer transition

Figure 9.9
Typical characteristics of boundary layer thickness and wall shear stress for laminar and turbulent boundary layers.

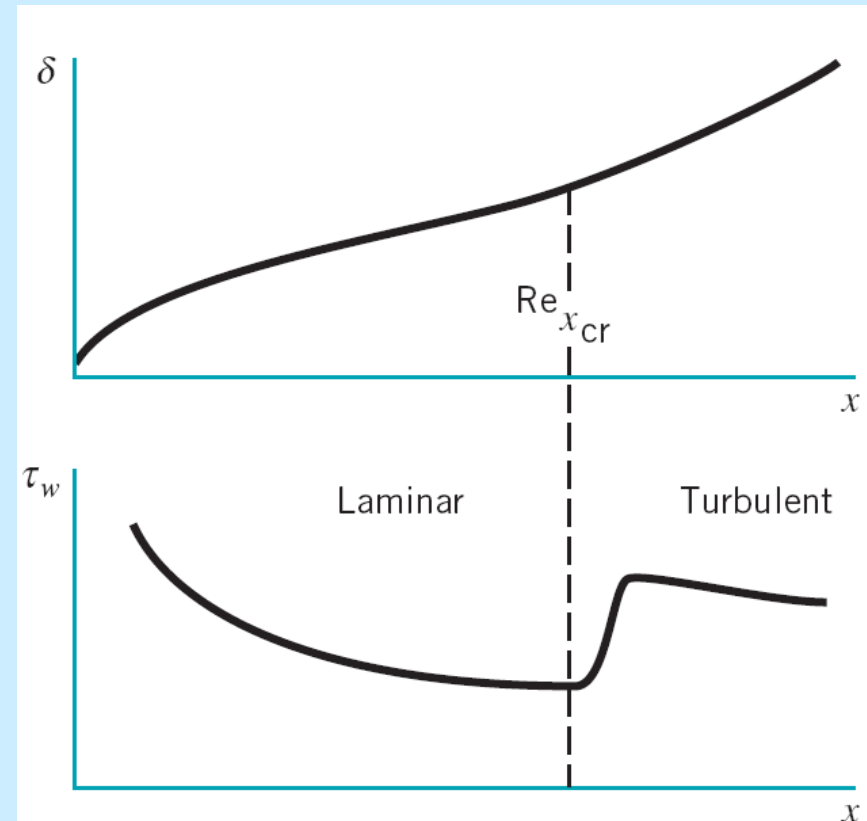




Figure 9.13 (p. 483)
 Turbulent spots and the transition from laminar to turbulent boundary layer flow on a flat plate. Flow from left to right. (Photograph courtesy of B. Cantwell, Stanford University.)

V9.5 Transition on flat plate

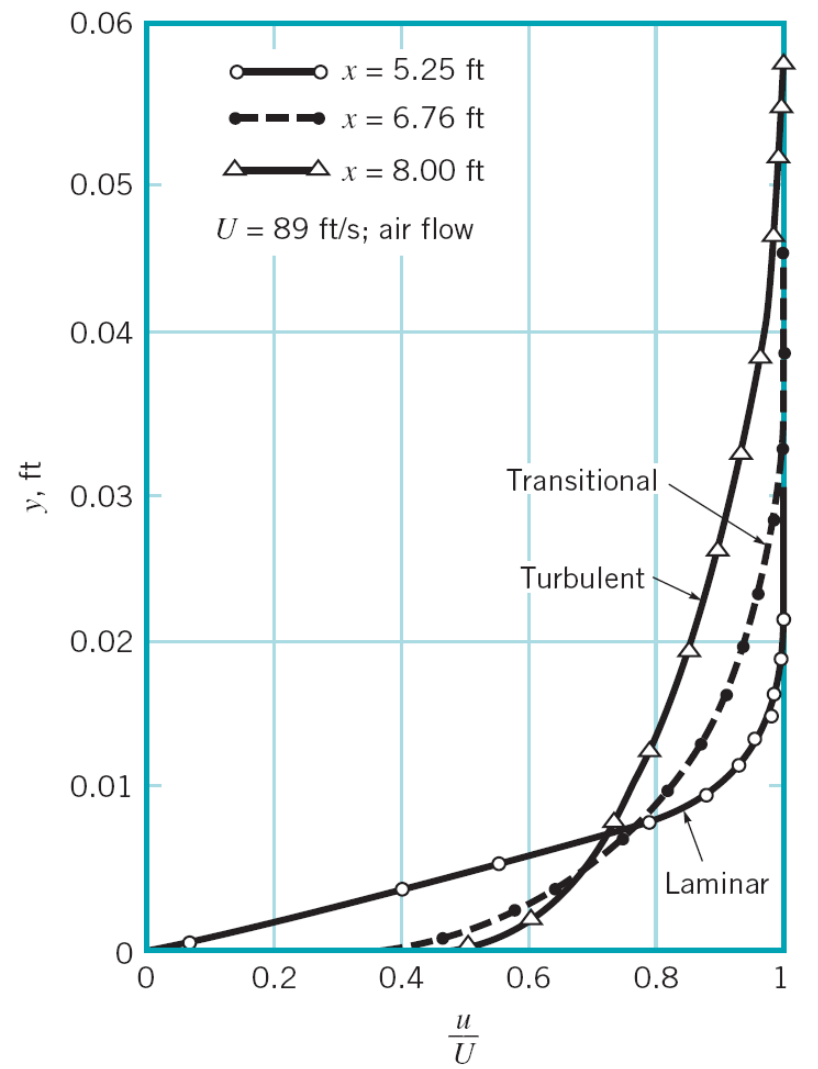
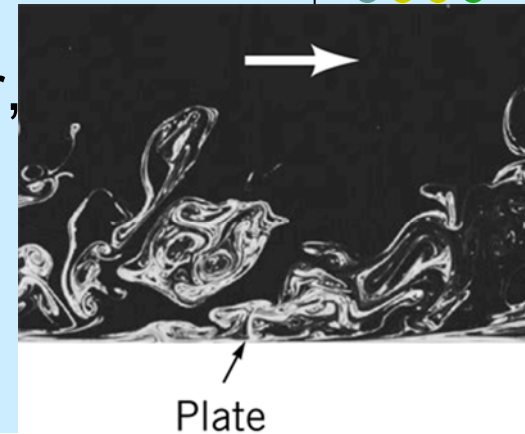


Figure 9.14 (p. 484)
 Typical boundary layer profiles on a flat plate for laminar, transitional, and turbulent flow (Ref. 1).

9.2.5 Turbulent Boundary Layer Flow

- The structure of turbulent boundary layer flow is very complex, random, and irregular, with significant cross-stream mixing.
- Empirical power-law velocity profile is a reasonable approximation.



Example 9.6

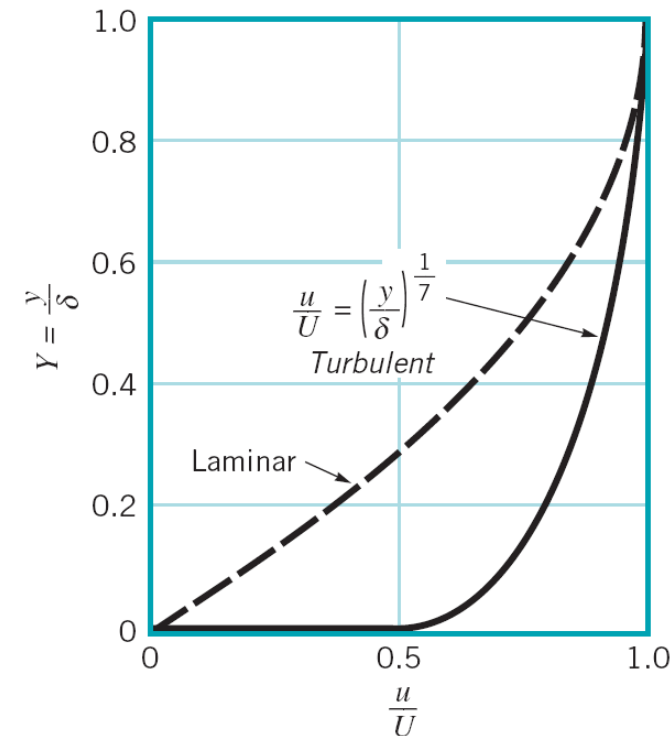
To begin with the momentum integral equation:

$$\tau_w = \rho U^2 \frac{d\theta}{dx}$$

Assume $\frac{u}{U} = \left(\frac{y}{\delta}\right)^{1/7} = Y^{1/7} \begin{cases} Y = \frac{y}{\delta}, Y < 1 \\ u = U, Y > 1 \end{cases}$

and the experimentally determined formula:

$$\tau_w = 0.0225 \rho U^2 \left(\frac{\nu}{U\delta}\right)^{1/4} \quad (1)$$



$$\tau_w = \rho U^2 \frac{d\theta}{dx}$$

$$\theta = \int_0^{\infty} \frac{u}{U} \left(1 - \frac{u}{U}\right) dy = \delta \int_0^1 \frac{u}{U} \left(1 - \frac{u}{U}\right) dY = \delta \int_0^1 Y^{1/7} \left(1 - Y^{1/7}\right) dY = \frac{7}{72} \delta$$



(2)

where δ is still unknown.

To determine δ , we combine Eq. 1 with Eq. 2 to get the ODE:

$$0.0225 \rho U^2 \left(\frac{\nu}{U\delta}\right)^{1/4} = \frac{7}{72} \rho U^2 \frac{d\delta}{dx} \quad \text{or} \quad \delta^{1/4} d\delta = 0.231 \left(\frac{\nu}{U}\right)^{1/4} dx$$

with BC: $\delta = 0$ at $x = 0$, we obtain

$$\delta = 0.370 \left(\frac{\nu}{U}\right)^{1/5} x^{4/5}, \quad \text{or} \quad \frac{\delta}{x} = \frac{0.370}{\text{Re}_x^{1/5}}$$

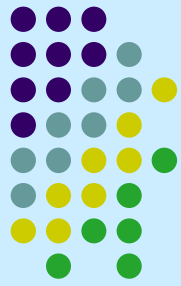
$$\delta^* = \int_0^{\infty} \left(1 - \frac{u}{U}\right) dy = \delta \int_0^1 \left(1 - \frac{u}{U}\right) dY = \delta \int_0^1 \left(1 - Y^{1/7}\right) dY = \frac{\delta}{8} = 0.0463 \left(\frac{\nu}{U}\right)^{1/5} x^{4/5}$$

$$\theta = \frac{\delta}{72} = 0.036 \left(\frac{\nu}{U}\right)^{1/5} x^{4/5}, \quad \theta < \delta^* < \delta$$

$$\tau_w = 0.0225 \rho U^2 \left[\frac{\nu}{U 0.37 (\nu/U)^{1/5} x^{4/5}} \right]^{1/4} = \frac{0.0288 \rho U^2}{\text{Re}_x^{1/5}}$$

$$D_f = \int_0^{\ell} b \tau_w dx = b 0.0288 \rho U^2 \int_0^{\ell} \left(\frac{\nu}{U x} \right)^{1/5} dx = 0.036 \rho U^2 \frac{A}{\text{Re}_\ell^{1/5}}, \quad A = b\ell$$

$$C_{Df} = \frac{D_f}{\frac{1}{2} \rho U^2 A} = \frac{0.072}{\text{Re}_\ell^{1/5}}$$

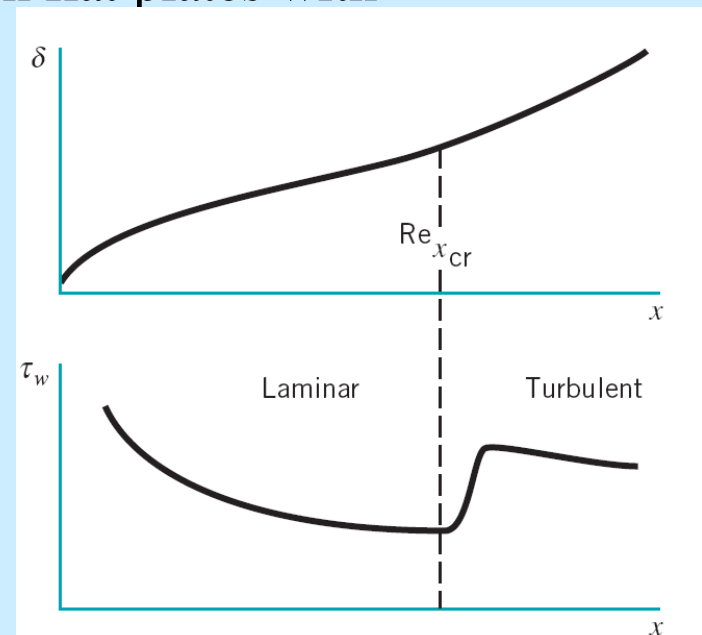


Note: The above results are valid for smooth flat plates with

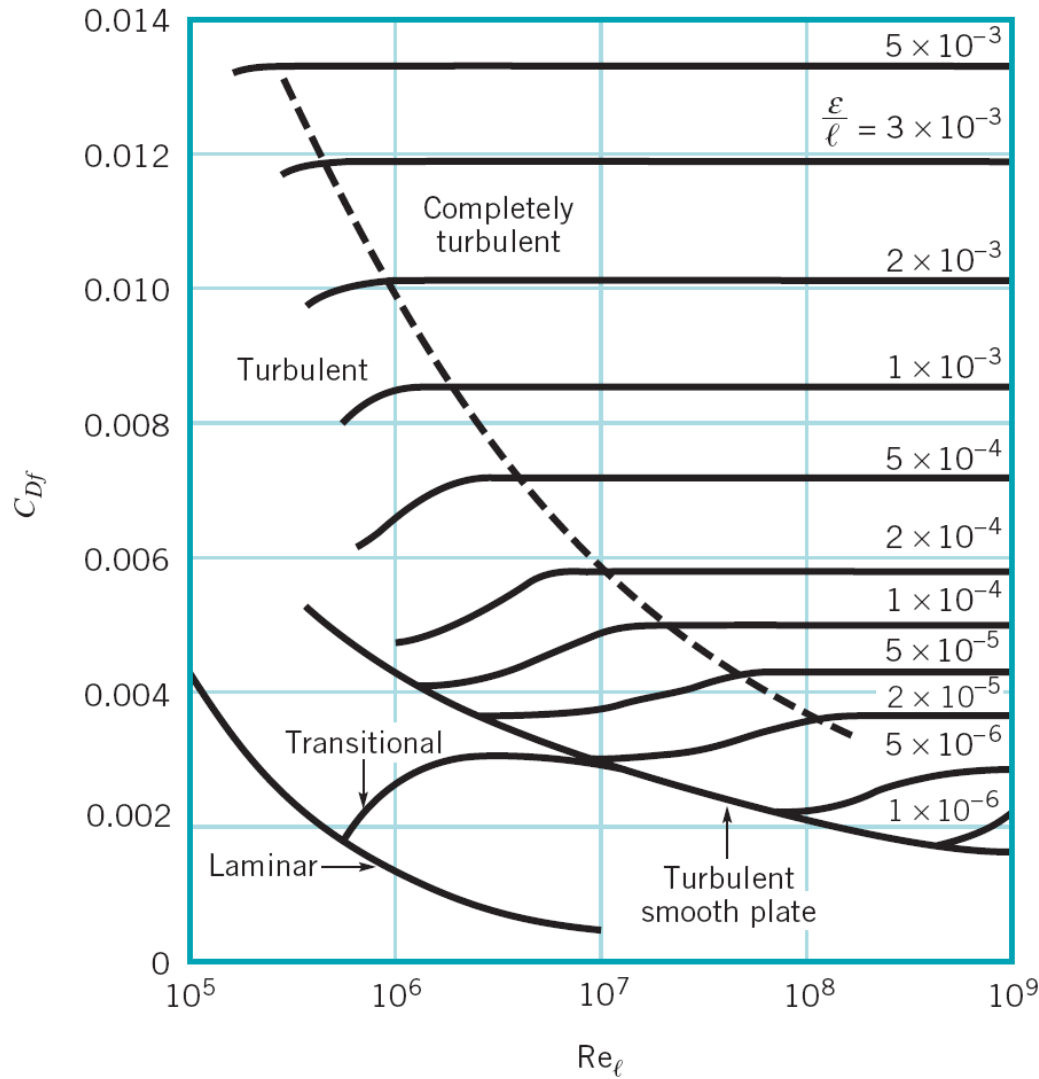
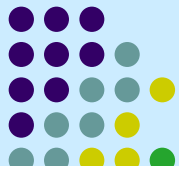
$$5 \times 10^5 < \text{Re}_x < 10^7$$

Turbulent B.L.: $\delta \propto x^{4/5}, \tau_w \propto x^{-1/5}$

Laminar B.L.: $\delta \propto x^{1/2}, \tau_w \propto x^{-1/2}$



Friction drag coefficient for a flat plate



- Although Fig. 9.15 is similar with Moody diagram (pipe flow) of Fig. 8.23, **the mechanisms are quite different.**

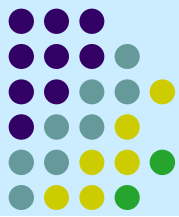
For fully developed pipe flow, fluid inertia remains constant and the flow is balanced between pressure forces and viscous forces.

For flat plate boundary layer flow, pressure remains constant and the flow is balanced between inertia effects and viscous forces.

Figure 9.15

Friction drag coefficient for a flat plate parallel to the upstream flow.

Empirical equations for C_{Df}



■ TABLE 9.3

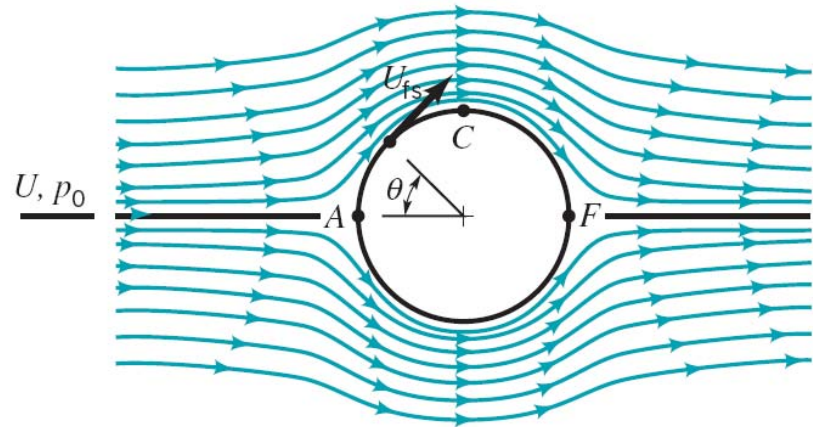
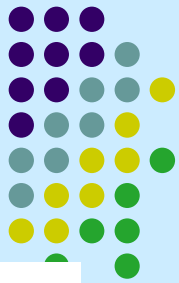
Empirical Equations for the Flat Plate Drag Coefficient (Ref. 1)

Equation	Flow Conditions
$C_{Df} = 1.328/(\text{Re}_\ell)^{0.5}$	Laminar flow
$C_{Df} = 0.455/(\log \text{Re}_\ell)^{2.58} - 1700/\text{Re}_\ell$	Transitional with $\text{Re}_{x_{cr}} = 5 \times 10^5$
$C_{Df} = 0.455/(\log \text{Re}_\ell)^{2.58}$	Turbulent, smooth plate
$C_{Df} = [1.89 - 1.62 \log(\varepsilon/\ell)]^{-2.5}$	Completely turbulent

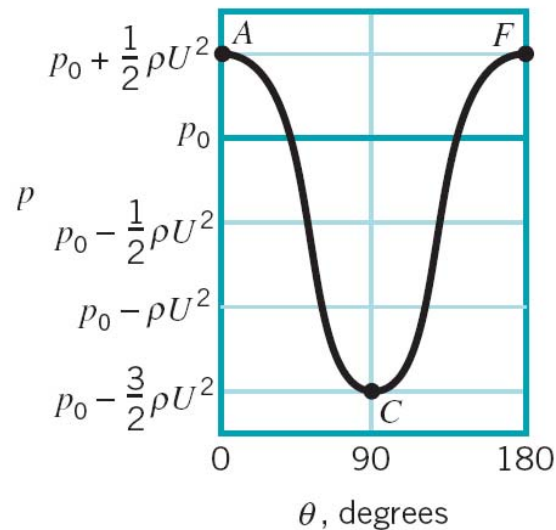
Example 9.7

9.2.6 Effects of Pressure Gradient

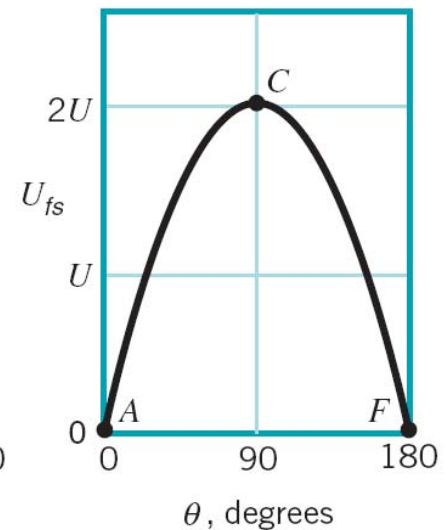
Inviscid flow over a cylinder



(a)

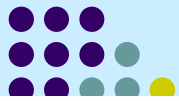


(b)



(c)

Viscous flow over a cylinder



- Viscous flow

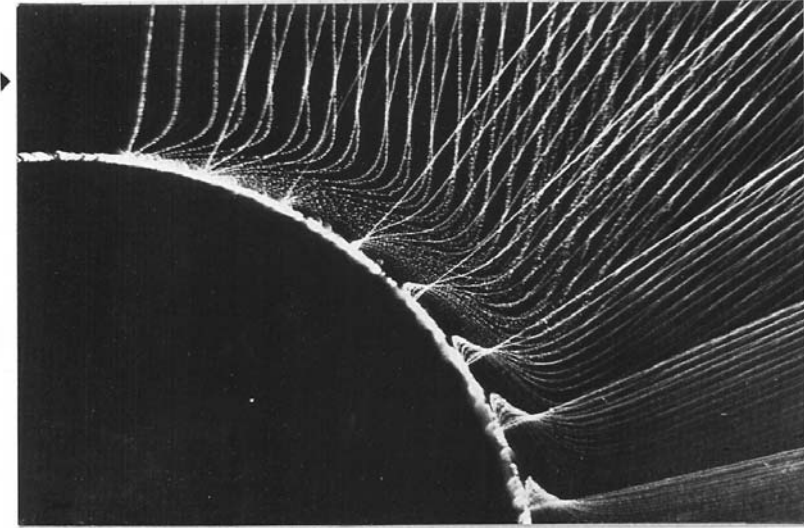
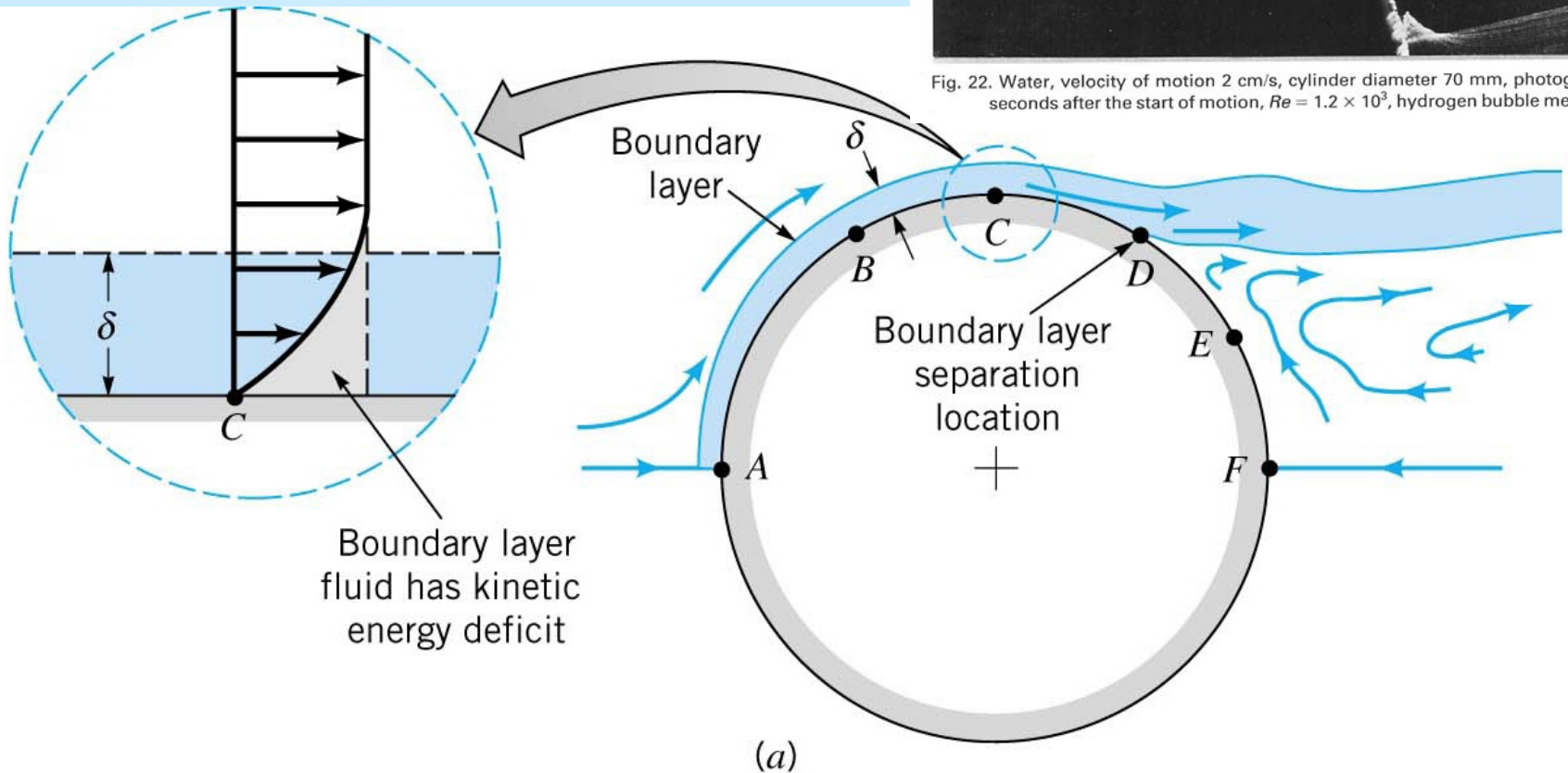
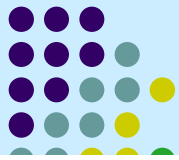


Fig. 22. Water, velocity of motion 2 cm/s, cylinder diameter 70 mm, photographed two seconds after the start of motion, $Re = 1.2 \times 10^3$, hydrogen bubble method.

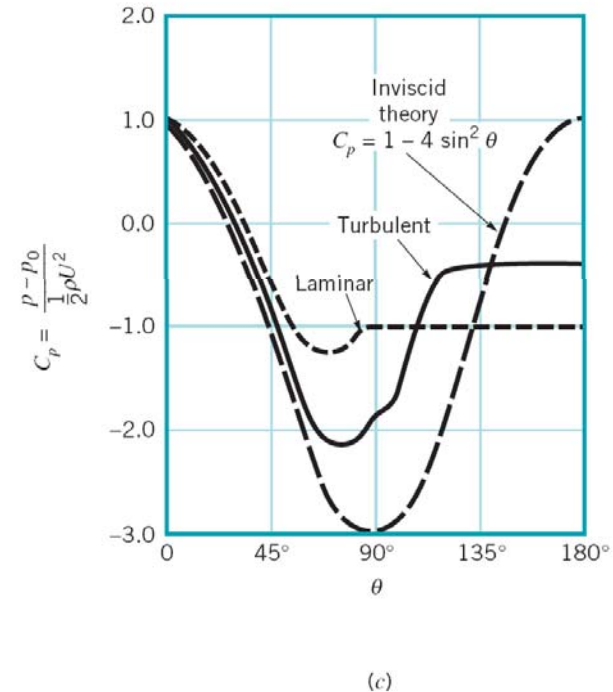
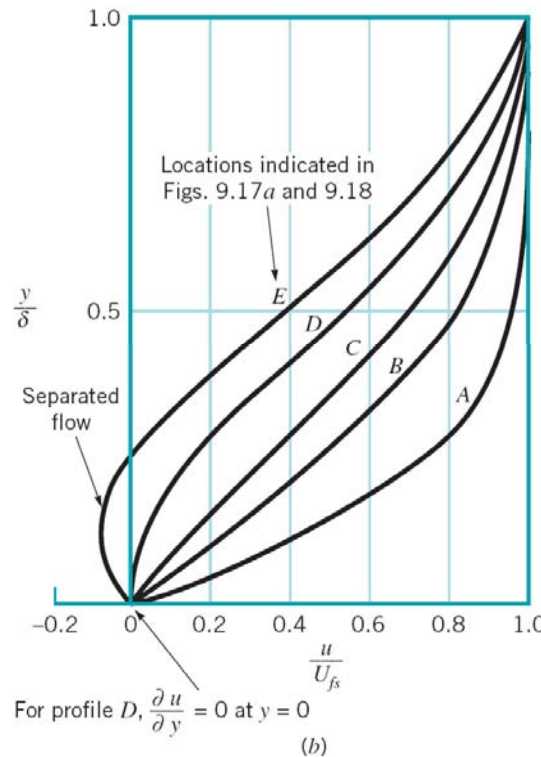
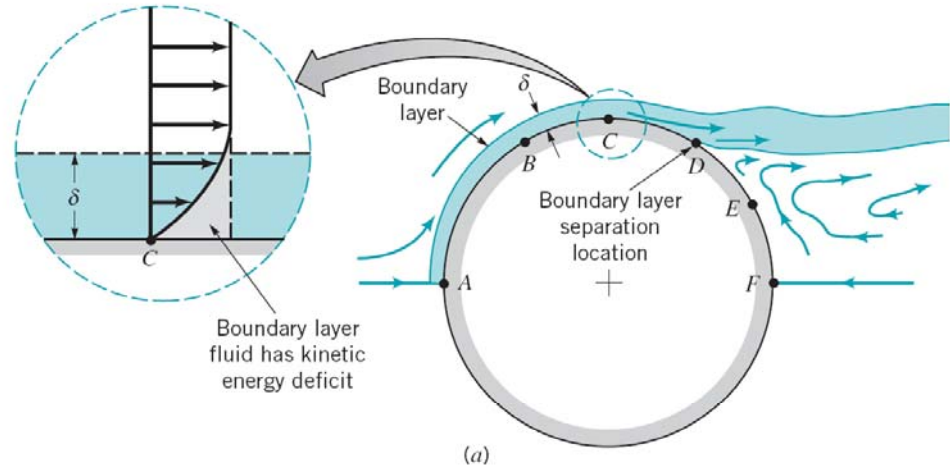


Viscous flow over cylinder: velocity-pressure

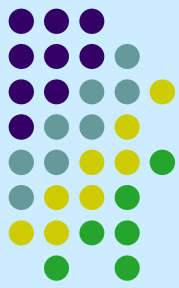


- Separated flow

- No matter how small the viscosity, provided it is not zero, there will be a boundary layer that separates from the surface, giving a drag that is, for the most part, independent of the value of μ .



9.2.7 Momentum-Integral Boundary Layer Equation with Nonzero Pressure Gradient



- Outside the boundary layer

$$p + \frac{\rho U_{fs}^2}{2} = \text{constant}$$

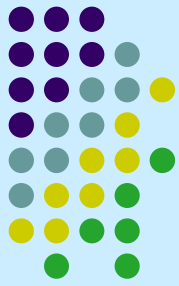
$$\frac{dp}{dx} = -\rho U_{fs} \frac{dU_{fs}}{dx} \quad (9.34)$$

- Momentum integral boundary layer equation

$$\tau_w = -\rho \frac{d}{dx} (U_{fs}^2 \theta) + \rho \delta^* U_{fs} \frac{dU_{fs}}{dx} \Leftrightarrow (\text{for } U = C, \tau_w = \rho U^2 \frac{d\theta}{dx}) \quad (9.35)$$

- This equation represents a balance between viscous forces (τ_w), pressure forces ($\frac{dp}{dx} = -\rho U_{fs} \frac{dU_{fs}}{dx}$), and the fluid momentum (θ).
- Eq. 9.35 can be used to provide information about the boundary layer thickness, wall shear stress, etc,

Derivation of equation (9.35)



$$\frac{\partial u}{\partial x} + \frac{\partial v}{\partial y} = 0 \quad (\text{a})$$

$$u \frac{\partial u}{\partial x} + v \frac{\partial u}{\partial y} = U \frac{\partial U}{\partial x} + \frac{1}{\rho} \frac{\partial \tau}{\partial y} \quad (\text{b})$$

$$(\text{b}) - (u - U)(\text{a})$$

$$-\frac{1}{\rho} \frac{\partial \tau}{\partial y} = \frac{\partial}{\partial x} (uU - u^2) + (U - u) \frac{\partial U}{\partial x} + \frac{\partial}{\partial y} (vU - vu)$$

$$\int_0^{\delta} -\frac{1}{\rho} \frac{\partial \tau}{\partial y} dy = \frac{\partial}{\partial x} \int_0^{\delta} u(U - u) dy + \frac{\partial U}{\partial x} \int_0^{\delta} (U - u) dy + \int_0^{\delta} \frac{\partial}{\partial y} (vU - vu) dy$$

$v=0$ at $y=0, \delta$

$$\int_0^{\delta} -\frac{1}{\rho} \frac{\partial \tau}{\partial y} dy = \frac{\partial}{\partial x} \int_0^{\delta} u(U - u) dy + \frac{\partial U}{\partial x} \int_0^{\delta} (U - u) dy$$

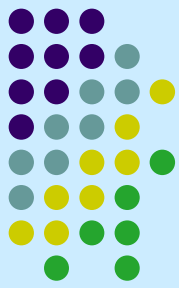
$$\frac{\tau}{\rho} = \frac{\partial}{\partial x} \int_0^{\delta} u(U - u) dy + \frac{\partial U}{\partial x} \int_0^{\delta} (U - u) dy$$

$$= \frac{\partial}{\partial x} \left[U^2 \int_0^{\delta} \frac{u}{U} \left(1 - \frac{u}{U} \right) dy + \frac{\partial U}{\partial x} U \int_0^{\delta} \left(1 - \frac{u}{U} \right) dy \right]$$

$$= \frac{\partial}{\partial x} (U^2 \theta) + U \delta^* \frac{\partial U}{\partial x}$$

(9.35)

9.3 Drag



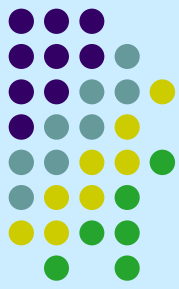
- Any object moving through a fluid will experience a drag D -- a net force in the direction of flow due to pressure (**pressure drag**) and shear stress (**friction drag**) on the surface of the object.

Drag coefficient:

$$C_D = \frac{D}{\frac{1}{2} \rho U^2 A} = \phi(\text{shape, Re, Ma, Fr, } \varepsilon / \ell)$$

These are determined experimentally, and very few can be obtained analytically.

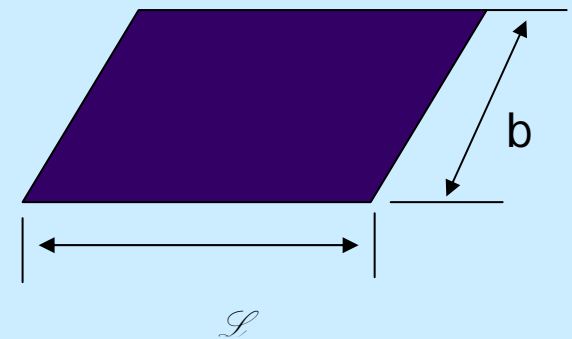
9.3.1 Friction Drag



- Drag due to the shear stress τ_w , on the object.
- For large Re, the friction drag is generally smaller than pressure drag.
- However, for highly streamlined bodies or for low Reynolds number flow, most of the drag may be due to friction drag.
- Drag on a plate of width b and length l

$$D_f = \frac{1}{2} \rho U^2 b l C_{Df}$$

where C_{Df} is the friction drag coefficient.

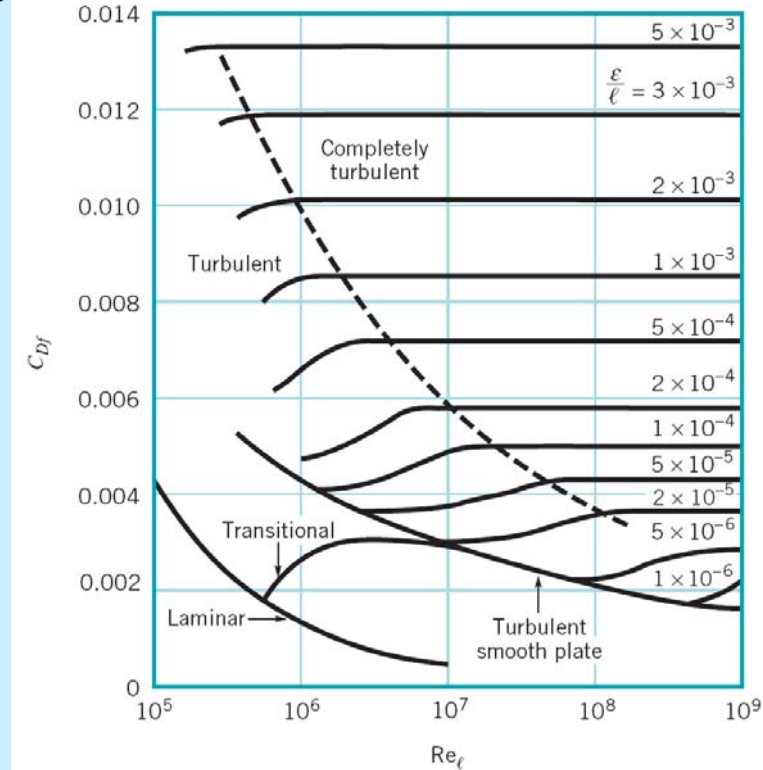
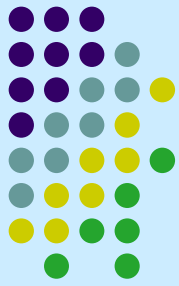


Friction Drag

For laminar flow, C_{Df} is independent of $\frac{\varepsilon}{D}$

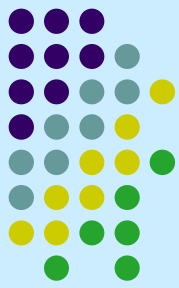
For turbulent flow, C_{Df} is function of $\frac{\varepsilon}{D}$

C_{Df} along the surface of a curved body is quite difficult to obtain



Example 9.8 Friction drag coeff. for a cylinder

9.3.2 Pressure Drag

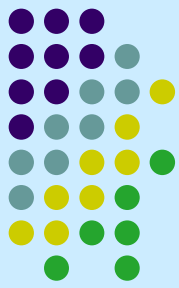


- Drag due to pressure on the object.
- **Pressure drag** – also called **form drag** because of its strong dependency on the shape or form of the object.

$$D_p = \int p \cos \theta dA \quad C_p = \frac{p - p_0}{\frac{1}{2} \rho U^2} : \text{pressure coefficient}$$

$$C_{Dp} = \frac{D_p}{\frac{1}{2} \rho U^2 A} = \frac{\int p \cos \theta dA}{\frac{1}{2} \rho U^2 A} = \frac{\int C_p \cos \theta dA}{A} \quad p_0: \text{reference pressure}$$

Pressure drag--Large Reynolds number



For large Reynolds number, (inertial effect \square viscous effect)

$$p - p_0 \propto \frac{1}{2} \rho U^2 \quad (\text{dynamic pressure})$$

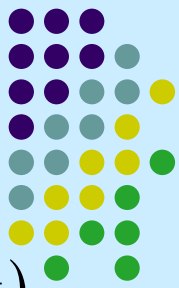
$$D_p = \int p \cos \theta dA \quad C_p = \frac{p - p_0}{\rho U^2 / 2}: \quad \text{pressure coefficient}$$

$$C_{Dp} = \frac{D_p}{\frac{1}{2} \rho U^2 A} = \frac{\int p \cos \theta dA}{\frac{1}{2} \rho U^2 A} = \frac{\int C_p \cos \theta dA}{A}$$

Therefore, C_p is independent of Reynolds number,

C_{Dp} is also independent of Reynolds number ($\text{Re} \square 1$)

Pressure drag--low Reynolds number



For very small Reynolds number (inertial effect \ll viscous effect)

$$\left\{ \begin{array}{l} \Delta p \propto \mu \frac{U}{l} \quad (\text{viscous stress}) \\ \tau_w \propto \mu \frac{U}{l} \end{array} \right. \quad C_{Dp} = \frac{D_p}{\frac{1}{2} \rho U^2 A} = \frac{\mu \frac{U}{l}}{\frac{1}{2} \rho U^2} = \frac{\mu}{\rho U l} = \frac{1}{\text{Re}}$$

Comparisons:

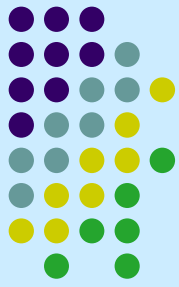
For laminar pipe flow $f = \frac{1}{\text{Re}}$

For large Reynolds number $f = \text{constant}$ (pipe flow)

Example 9.9 Pressure drag coeff. for a cylinder

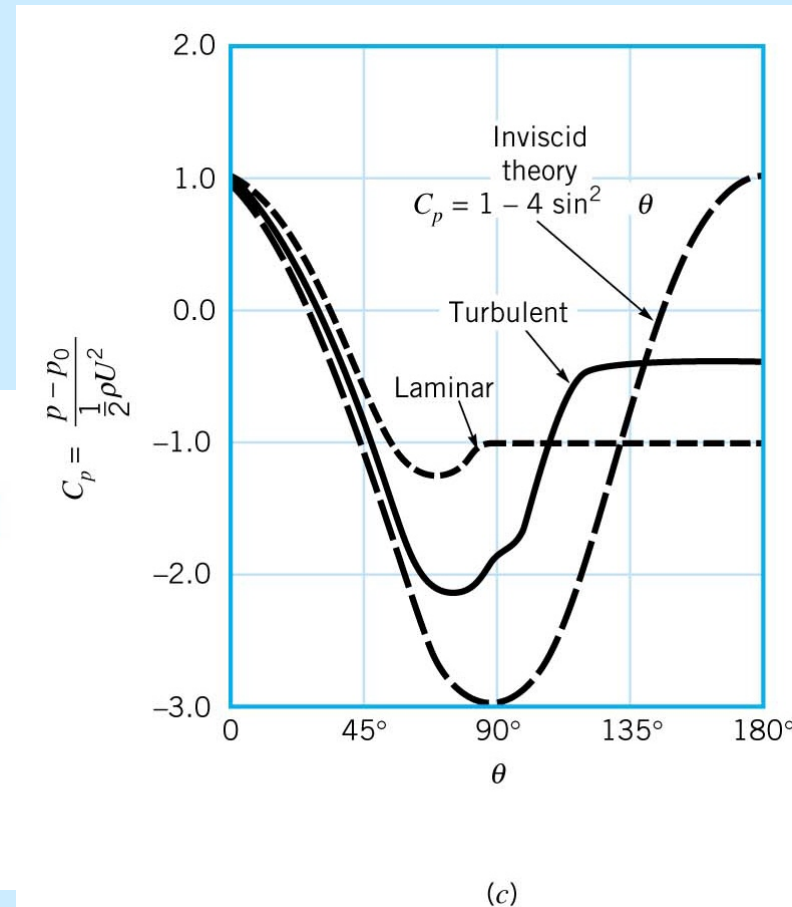
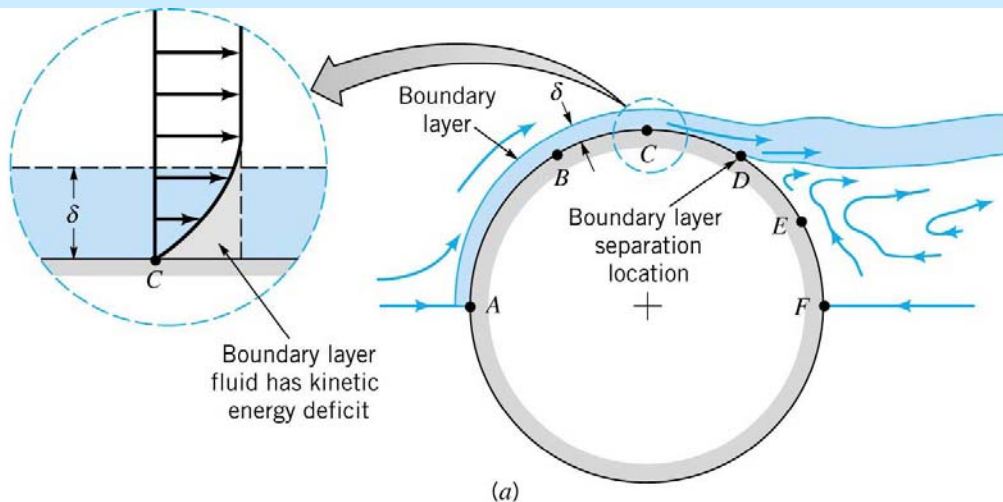
Viscosity Dependence

Inviscid, Viscous flows over object

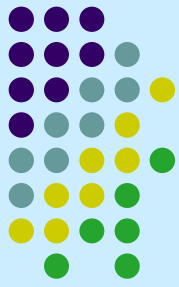


For $\mu = 0$, the pressure drag on any shaped object (symmetrical or not) in a steady flow would be zero.

For $\mu \neq 0$, the net pressure drag may be non-zero because of boundary layer separation.



9.3.3 Drag Coefficient Data and Examples



$$C_D = \phi \left(\text{shape}, \text{Re}, \text{Ma}, \text{Fr}, \frac{\varepsilon}{\ell} \right)$$

Shape Dependence

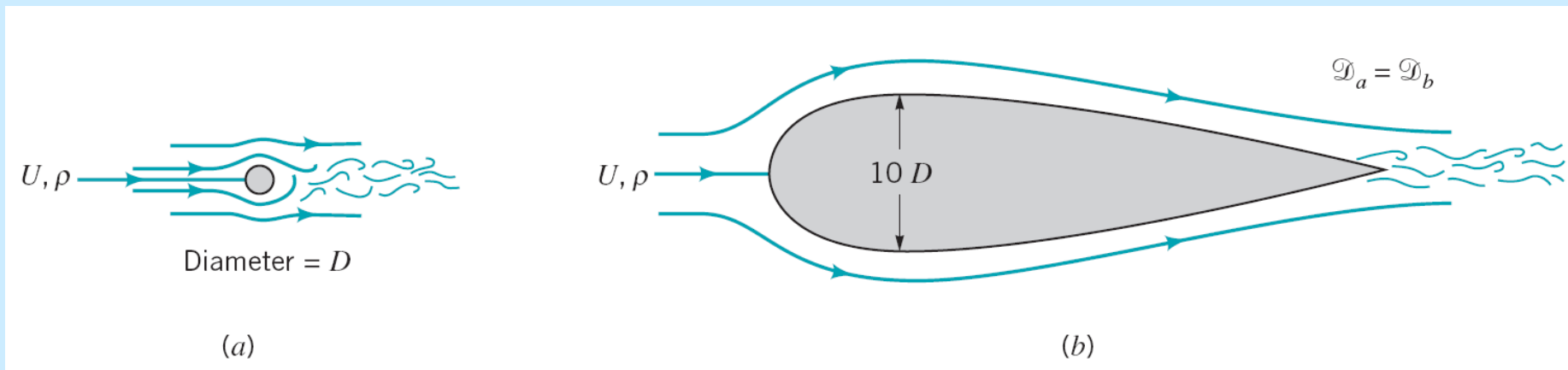


Figure 9.20

Two objects of considerably different size that have the same drag force:
(a) circular cylinder $C_D = 1.2$; (b) streamlined strut $C_D = 0.12$.

Shape Dependence

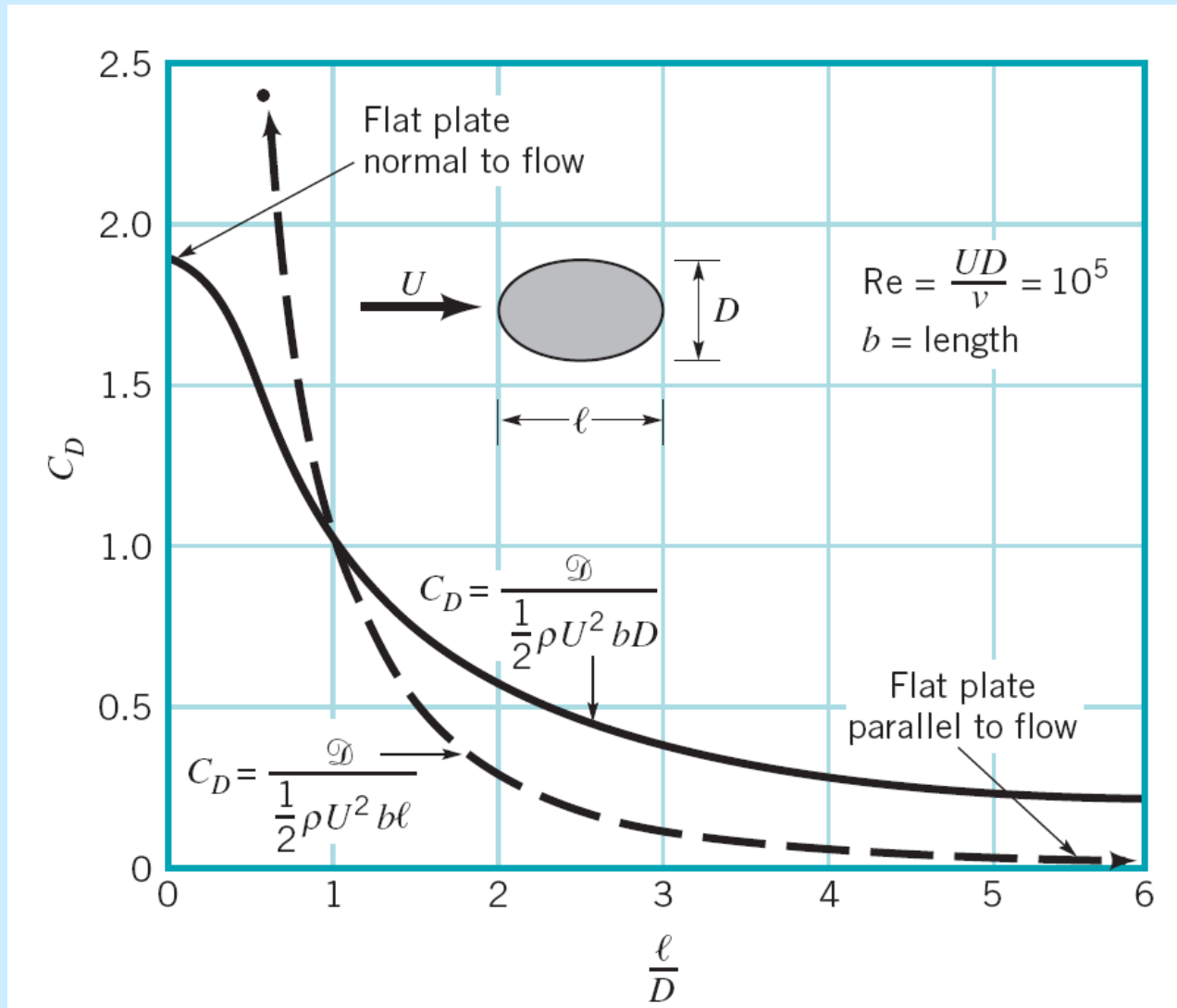
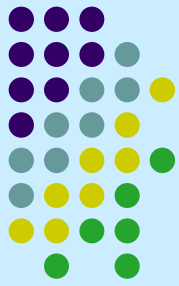


Figure 9.19

Drag coefficient for an ellipse with the characteristic area either the frontal area, $A = bD$, or the planform area, $A = b\ell$ (Ref. 5).

Reynolds Number Dependence

Low Reynolds number, $Re < 1$

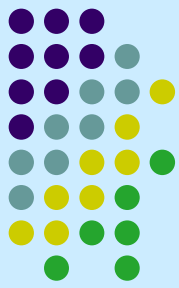
viscous force \approx pressure force

$$D = f(U, l, \mu)$$

From dimensional analysis

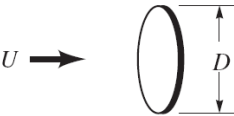
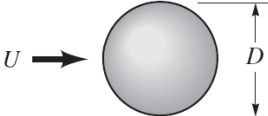
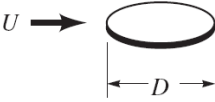
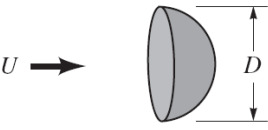
$$D = C\mu l U \quad [= C(\mu U / l) \cdot l^2]$$

$$C_D = \frac{D}{\frac{1}{2}\rho U^2 l^2} = \frac{2C\mu l U}{\rho U^2 l^2} = \frac{2C}{Re}, \quad Re = \frac{\rho U l}{\mu}$$



■ TABLE 9.4

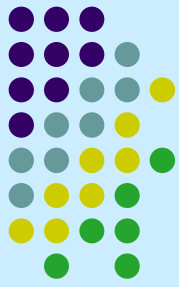
Low Reynolds Number Drag Coefficients (Ref. 7) ($Re = \rho U D / \mu, A = \pi D^2 / 4$)

Object	$C_D = \mathcal{D}/(\rho U^2 A/2)$ (for $Re \lesssim 1$)	Object	C_D
a. Circular disk normal to flow 	20.4/Re	c. Sphere 	24.0/Re
b. Circular disk parallel to flow 	13.6/Re	d. Hemisphere 	22.2/Re

Note: For $Re < 1$, streamlining increases the drag due to an increase in the area on which shear force act.

Ex 9.10: particle in the water dragged up by upward motion

V9.7 Skydiving practice



$D = 0.1\text{mm}$, $SG = 2.3$, to determine U

$$W = D + F_B$$

$$W = \gamma_{sand} \nabla = SG \gamma_{H_2O} \frac{\pi}{6} D^3, \quad F_B = \gamma_{H_2O} \nabla = \gamma_{H_2O} \frac{\pi}{6} D^3,$$

$$C_D = \frac{24}{\text{Re}} \quad (\text{For } \text{Re} < 1)$$

$$D = \frac{1}{2} \rho_{H_2O} U^2 \frac{\pi}{4} D^2 C_D = \frac{1}{2} \rho_{H_2O} U^2 \frac{\pi}{4} D^2 \left(\frac{24}{\rho_{H_2O} U D / \mu_{H_2O}} \right) = 3\pi \mu_{H_2O} U D$$

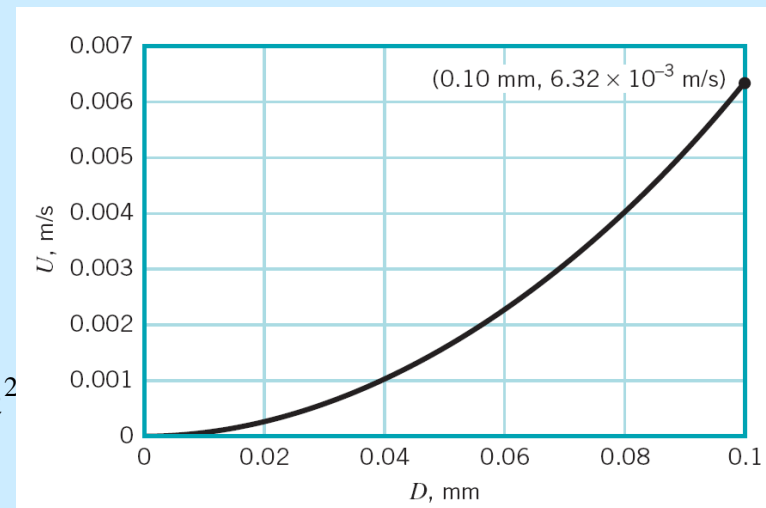
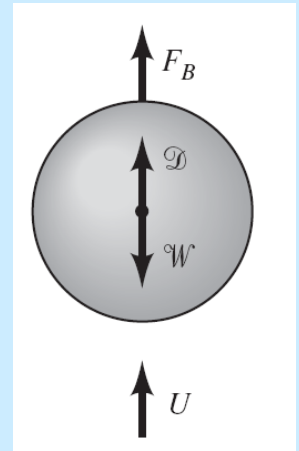
$$\therefore SG \gamma_{H_2O} \frac{\pi}{6} D^3 = 3\pi \mu_{H_2O} U D + \gamma_{H_2O} \frac{\pi}{6} D^3$$

$$\gamma = \rho g$$

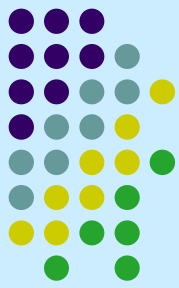
$$U = \frac{(SG \rho_{H_2O} - \rho_{H_2O}) g D^2}{18\mu} = 6.32 \times 10^{-3} \text{ m/s}$$

For 15.6°C , $\rho_{H_2O} = 999 \text{ kg/m}^3$, $\mu_{H_2O} = 1.12 \times 10^{-3} \text{ N}\cdot\text{s/m}^2$

$$\text{Re} = \frac{\rho U D}{\mu} = 0.564 \quad (\text{Re} < 1)$$

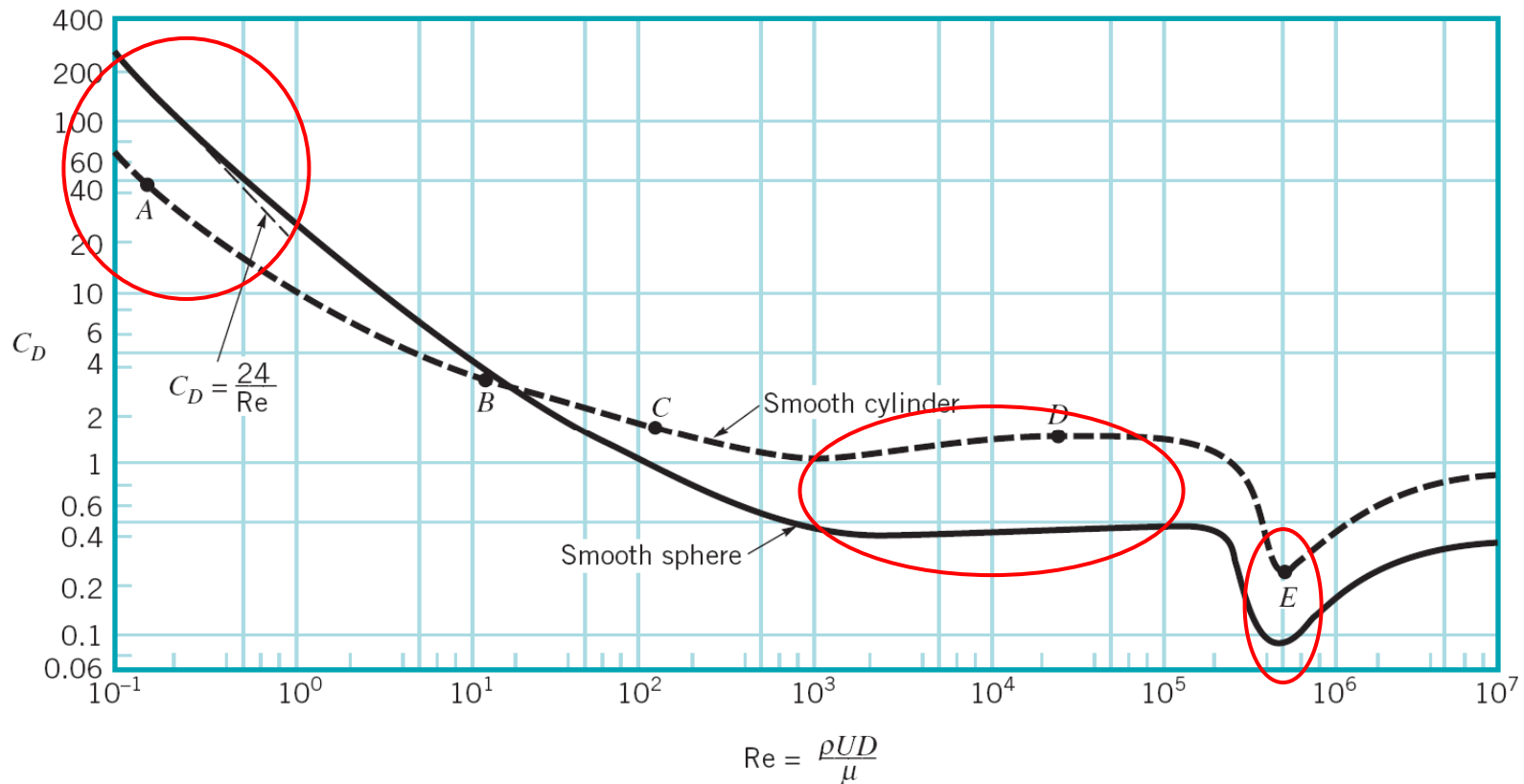


Moderate Reynolds Number C_D of cylinder and sphere



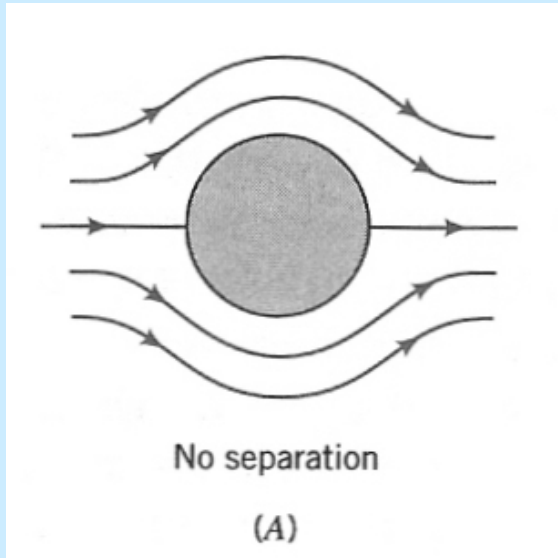
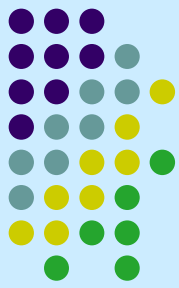
$Re < 10^3$ $C_D \propto Re^{-1/2}$ [$Re \uparrow$, $C_D \downarrow$ (not D)]

$10^3 < Re < 10^5$ $C_D \propto \text{constant}$

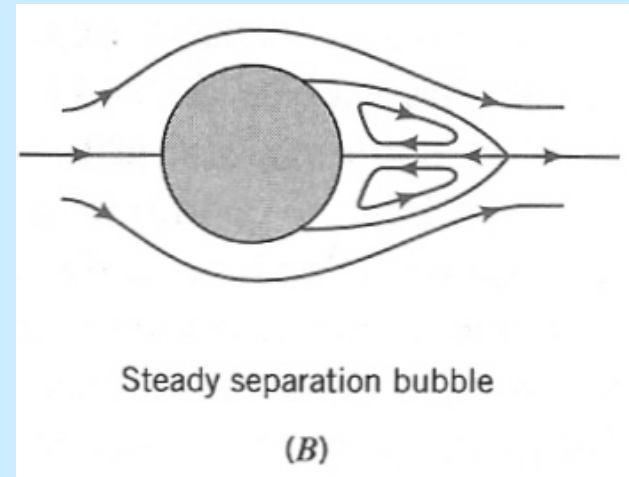


(a)

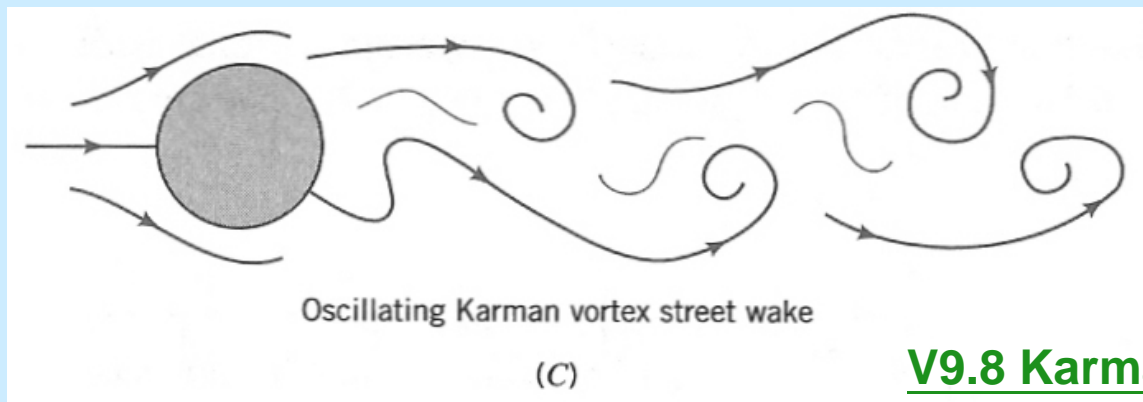
Flow over cylinder at various Reynolds number



$Re < 1$, no separation



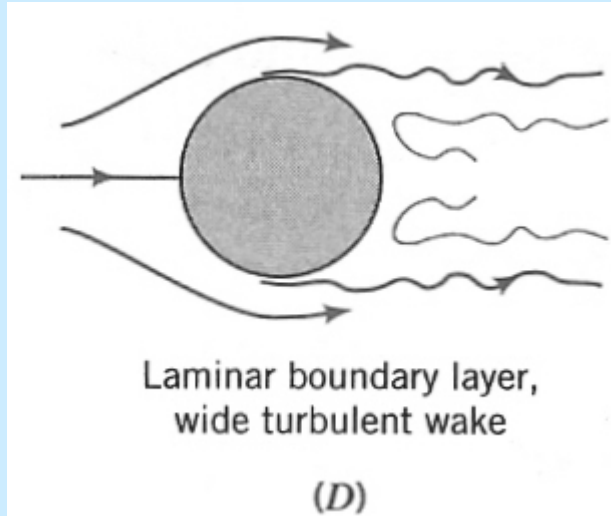
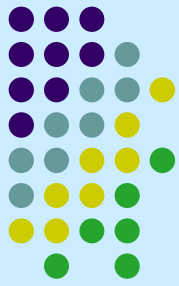
$Re \approx 10$, steady separation bubble



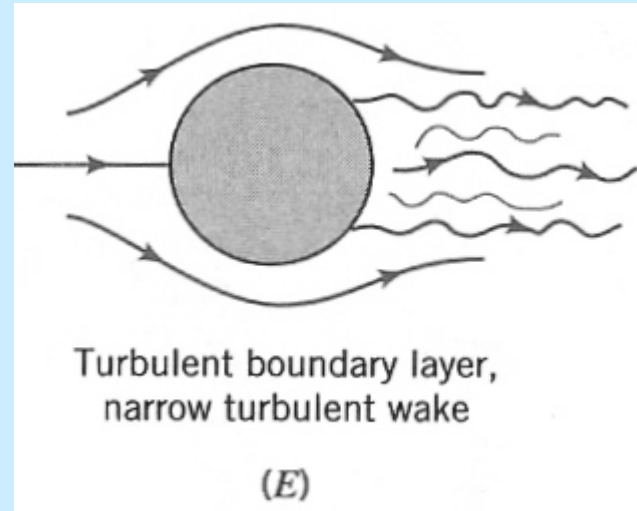
$Re \approx 100$, vortex shedding starts at $Re \approx 47$

[V9.8 Karman vortex street](#)

Flow over cylinder at various Reynolds number

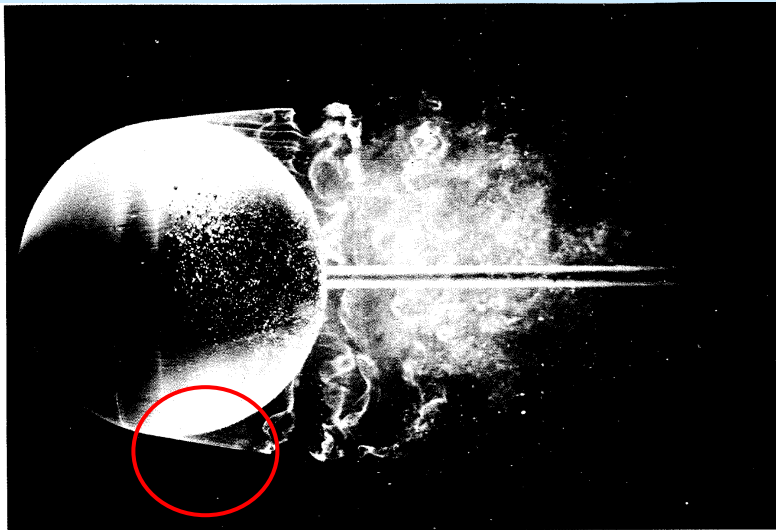


$$Re \approx 5 \times 10^4$$



$$Re \approx 4 \times 10^5$$

from M. Van Dyke, *An Album of Fluid Motion*



55. Instantaneous flow past a sphere at $R=15,000$. Dye in water shows a laminar boundary layer separating ahead of the equator and remaining laminar for almost one

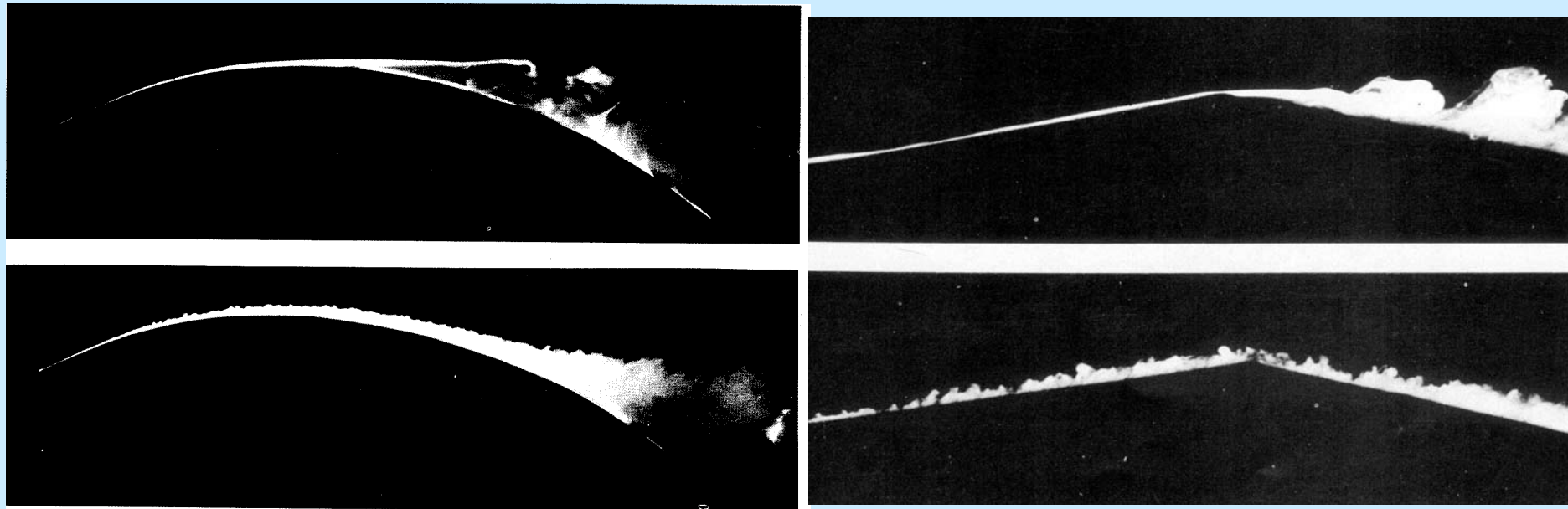
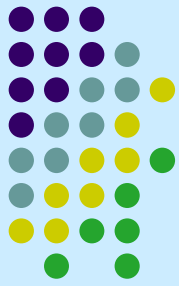
radius. It then becomes unstable and quickly turns turbulent. ONERA photograph, Werlé 1980



57. Instantaneous flow past a sphere at $R=30,000$ with a trip wire. A classical experiment of Prandtl and Wieselsberger is repeated here, using air bubbles in water. A wire hoop ahead of the equator trips the boundary layer. It becomes turbulent, so that it separates farther

rearward than if it were laminar (opposite page). The drag is thereby dramatically reduced, in a way that occurs naturally on a smooth sphere only at a Reynolds number ten times as great. ONERA photograph, Werlé 1980

Laminar and Turbulent Boundary Layer Separation



156. Comparison of laminar and turbulent boundary layers. The laminar boundary layer in the upper photograph separates from the crest of a convex surface (cf. figure 38), whereas the turbulent layer in the second

photograph remains attached; similar behavior is shown below for a sharp corner. (Cf. figures 55-58 for a sphere.) Titanium tetrachloride is painted on the forepart of the model in a wind tunnel. *Head 1982*

from M. Van Dyke, *An Album of Fluid Motion*

Drag of streamlined and blunt bodies

Drag coefficients

The different relations of C_D with Re for objects with various streamlining are illustrated in Fig. 9.22.

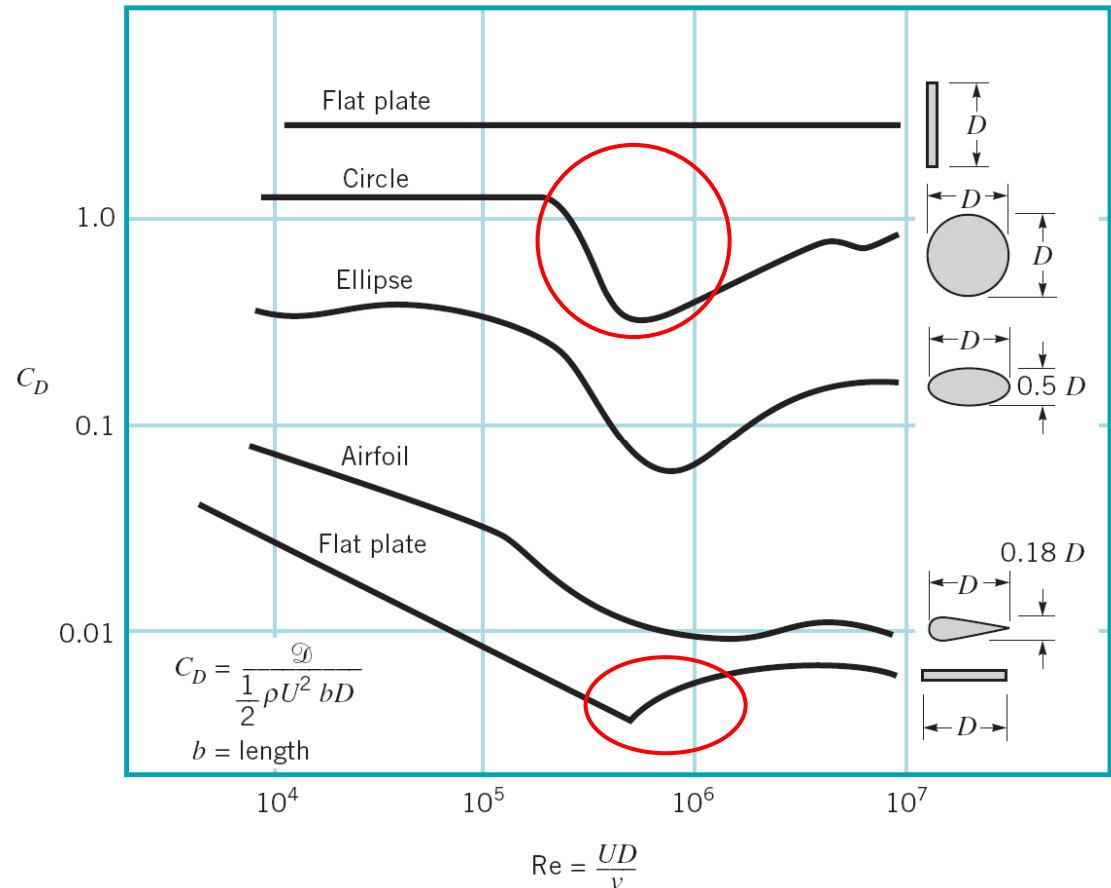
For streamlined bodies, $C_D \uparrow$ when the boundary layer becomes turbulent.
For blunt objects, $C_D \downarrow$ when the boundary layer becomes turbulent.

Note: In a portion of the range $10^5 < Re < 10^6$, the actual drag (not just C_D) decreases with increasing speed.

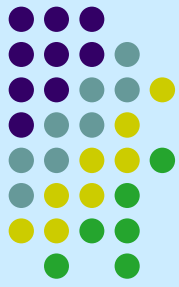
V9.9 Oscillating sign

V9.10 Flow past a flat plate

V9.11 Flow past an ellipse



Example 9.11 Terminal velocity of a falling object



$$W = D + F_B$$

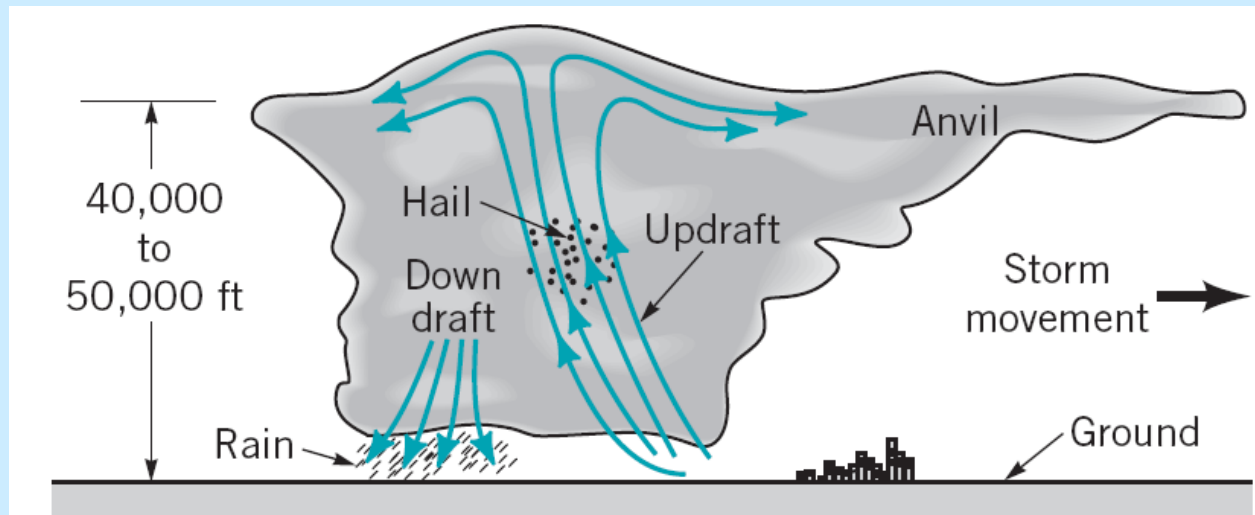
$$W = \gamma_{ice} \mathcal{V}, \quad F_B = \gamma_{air} \mathcal{V}$$

$$\frac{1}{2} \rho_{air} U^2 \frac{\pi}{4} D^2 C_D = W - F_B$$

$$\gamma_{ice} \square \gamma_{air} \quad \therefore W \square F_B$$

$$\frac{1}{2} \rho_{air} U^2 \frac{\pi}{4} D^2 C_D = W = \gamma_{ice} \mathcal{V}$$

$$U = \left(\frac{4 \rho_{ice} g D}{3 \rho_{air} C_D} \right)^{1/2}$$

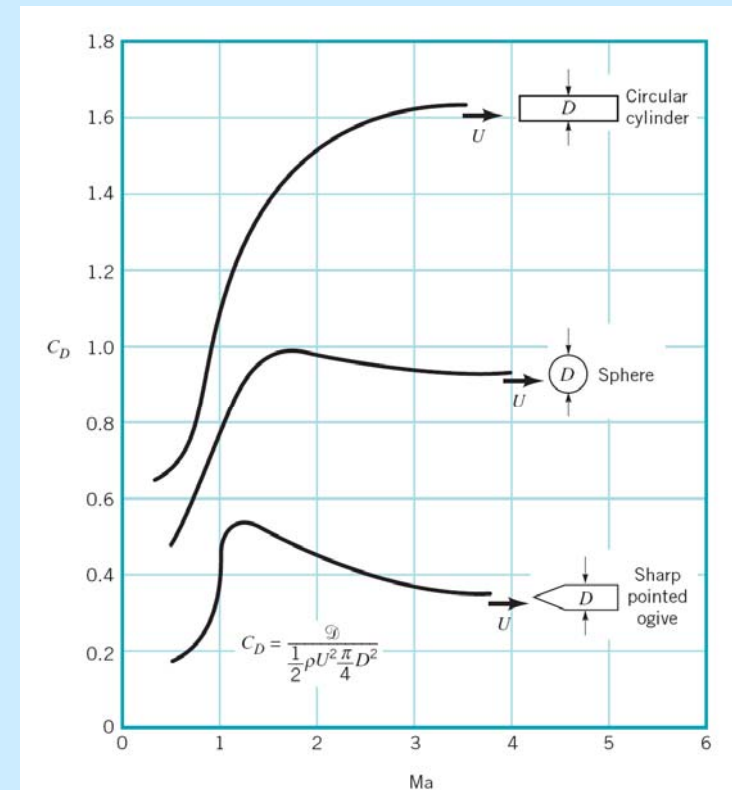
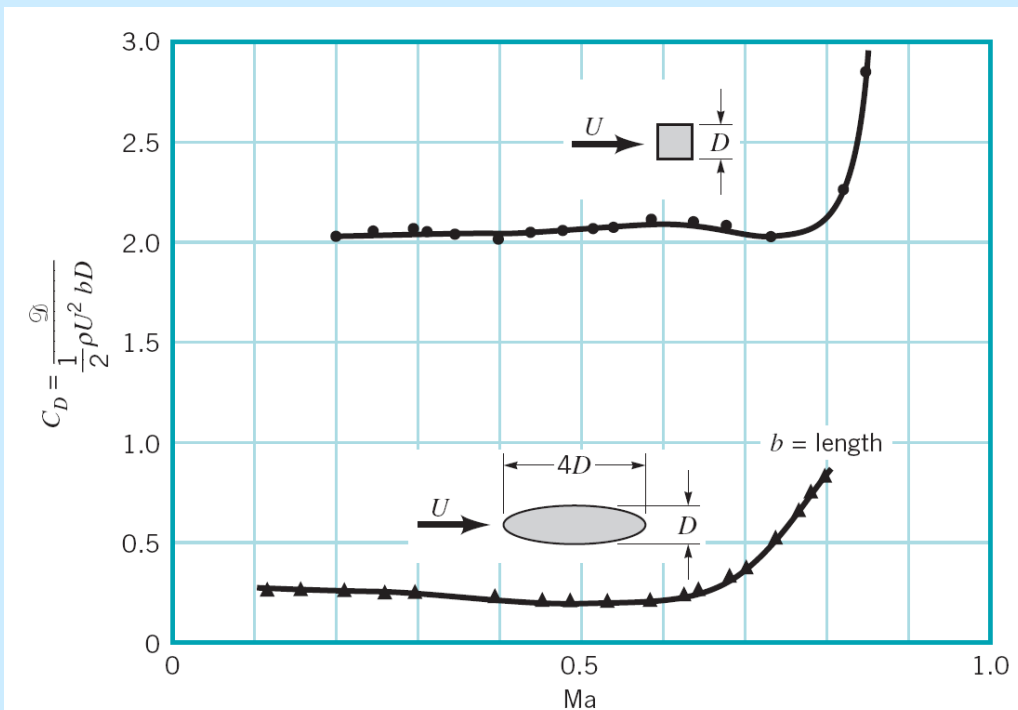
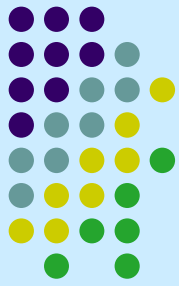


Compressibility Effects

When the compressibility effects become important

$$C_D = \phi(\text{Re}, \text{Ma})$$

- Notes:** 1. Compressibility effect is negligible for $\text{Ma} < 0.5$.
2. C_D increases dramatically near $\text{Ma} = 1$, due to the existence of shock wave.



Surface Roughness Effects



- Surface roughness influences drag when the boundary layer is turbulent, because it protrudes through the laminar sublayer and alters the wall shear stress.
- In addition, surface roughness can alter the transitional critical Re and change the net drag.

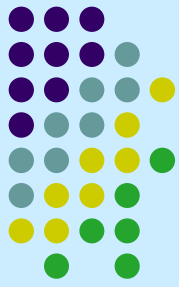
In general,

Streamlines bodies: $\frac{\varepsilon}{D} \uparrow \rightarrow C_D \uparrow$

Blunt bodies: $\frac{\varepsilon}{D} \uparrow \rightarrow C_D \square$ constant (pressure drag)

until transition to turbulence occurs and the wake region becomes considerably narrower so that the pressure drag drops. (Fig. 9.25)

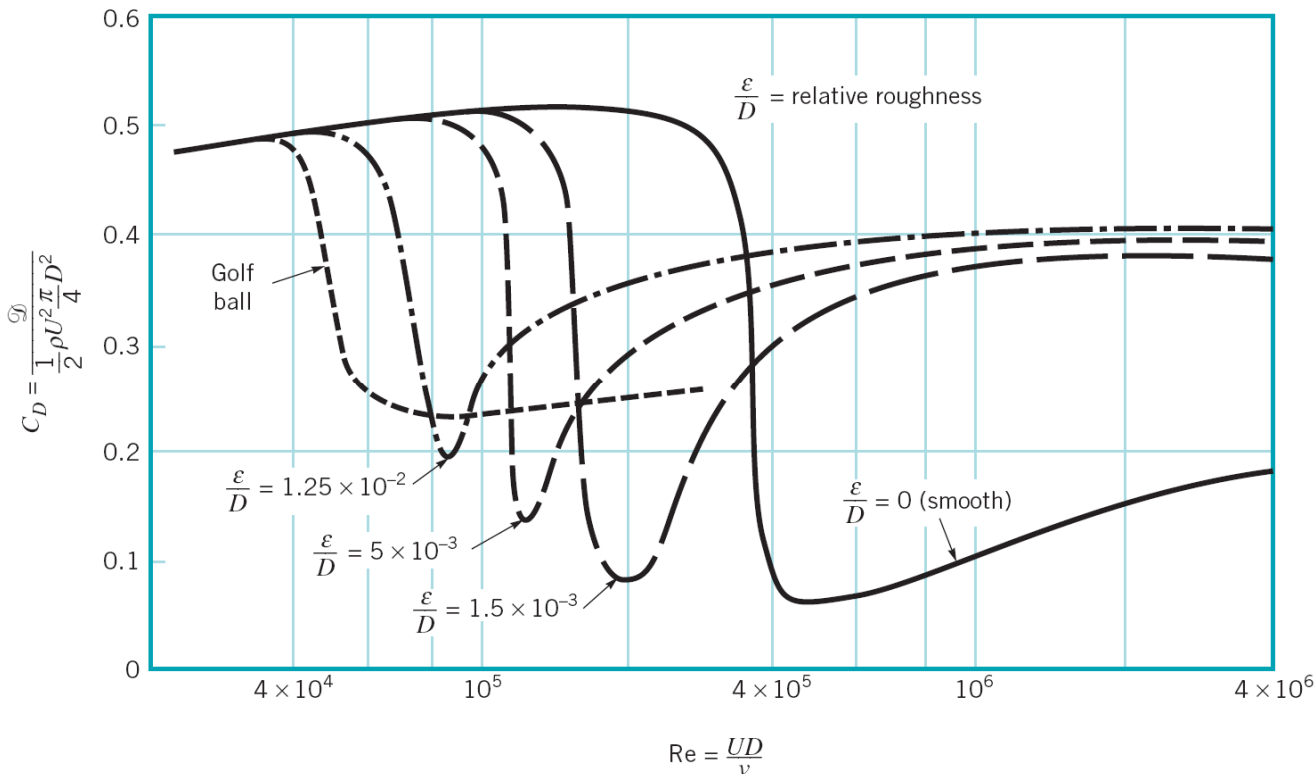
Surface Roughness



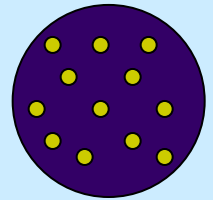
A well-hit golf ball has Re of $O(10^5)$, and the dimpled golf ball has a critical Reynolds number $4 \times 10^4 \rightarrow$ dimples reduce C_D

Table tennis Reynolds number is less than $4 \times 10^4 \rightarrow$ no need of dimples

Example 9.12 Effect of Surface Roughness for golf ball and table tennis ball

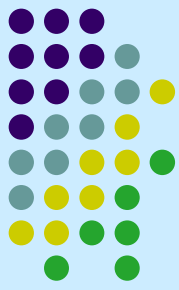


dimpled



$$\frac{C_{D,rough}}{C_{D,smooth}} = \frac{0.25}{0.5} = 0.5$$

Froude Number Effects (flows with free surface)



When the free surface is present, the wave-making effects becomes important, so that

$$C_D = \phi(\text{Re}, \text{Fr})$$

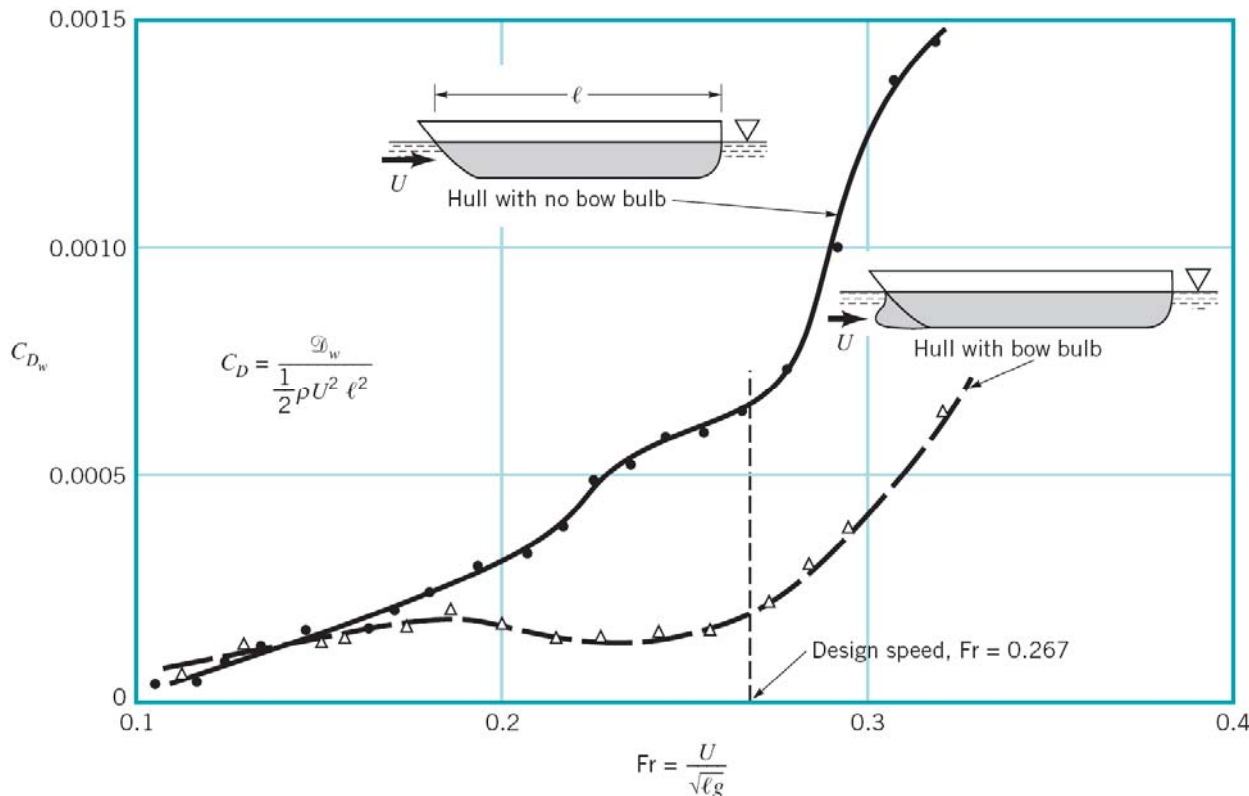
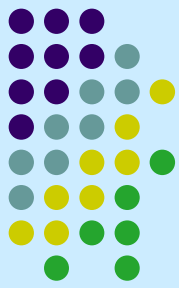


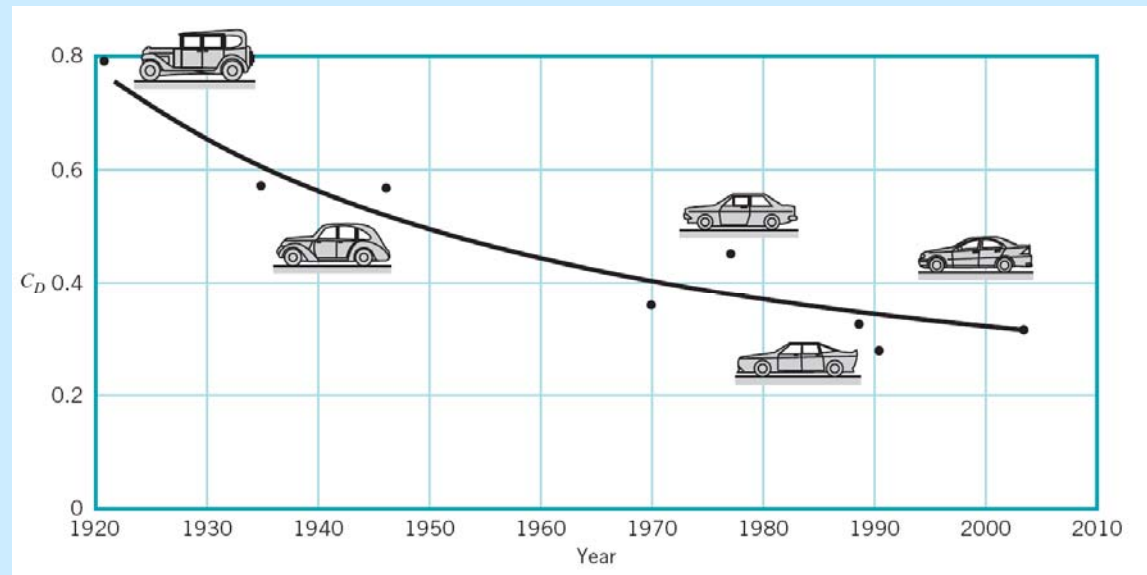
Figure 9.26 (p. 507)
Typical drag coefficient data as a function of Froude number and hull characteristics for that portion of the drag due to the generation of waves.

Composite body drag



- Approximate drag calculations for a complex body by treating it as composite collection of its various parts. e.g., drag on an airplane or an automobile.
- The contributions of the drag due to various portions of car (i.e., front end, windshield, roof, rear end, etc.) have been determined. As a result it is possible to predict the aerodynamic drag on cars of a wide variety of body styles (Fig. 9.27).

V9.14 Automobile streamlining



Example 9.13 Drag on a composite body

9.4 Lift (L)

9.4.1 Surface Pressure Distribution

- Lift -- a force that is normal to the free stream.

For aircraft, $L \uparrow$

For car, $L \downarrow$ for better traction and cornering ability

$$C_L = \frac{L}{\frac{1}{2} \rho U^2 A}, \quad C_L = \phi \left(\text{shape, Re, Ma, Fr, } \frac{\varepsilon}{l} \right)$$

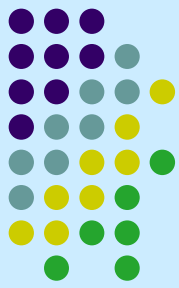
Froude no. – free surface present

ε is relatively unimportant

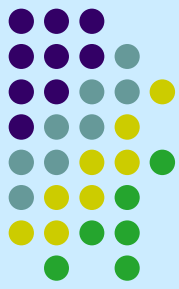
Ma is important for $\text{Ma} > 0.8$

Re effect is not great

The most important parameter that affects the lift coefficient is the shape of the object.



Surface Pressure Distribution



- Common lift-generating devices (airfoils, fans,...) operate at large Re . Most of the lift comes from the **surface pressure distribution**.
- For $Re < 1$, viscous effect and pressure are equally important to the lift (for minute insects and the swimming of microscopic organisms).

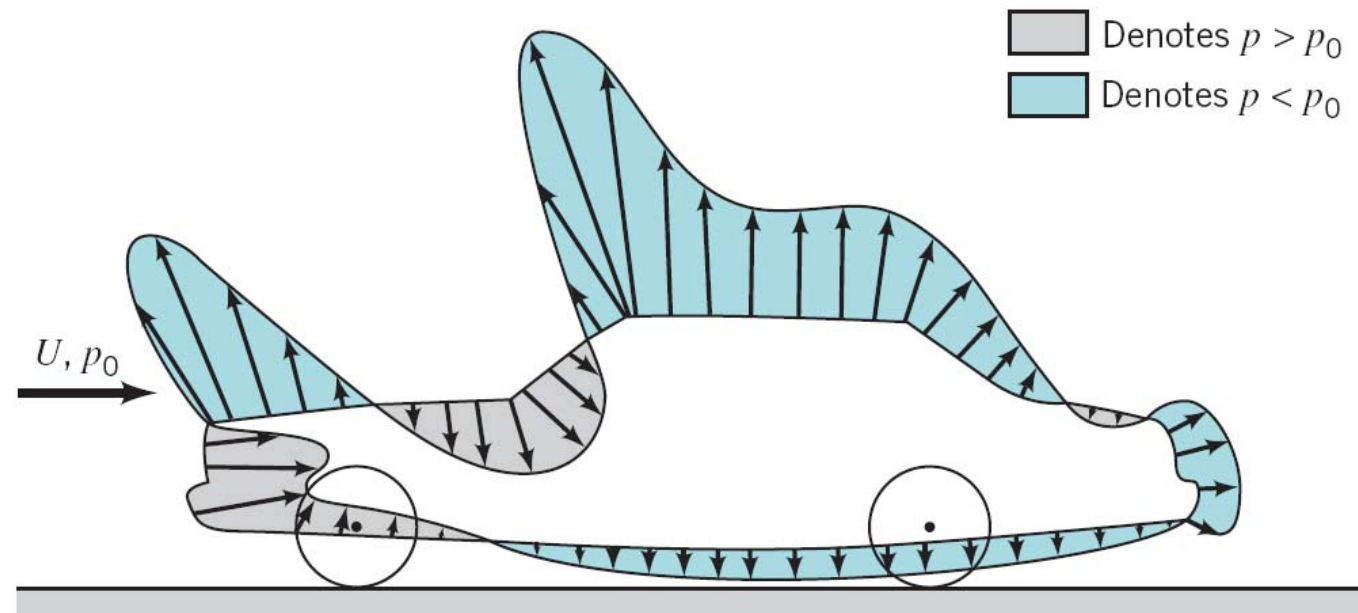
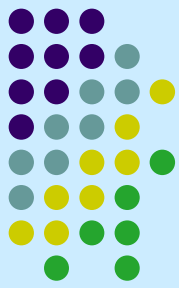


Figure 9.31
Pressure distribution
on the surface of an
automobile.

Example 9.14 Lift from pressure and shear distributions

Airfoil

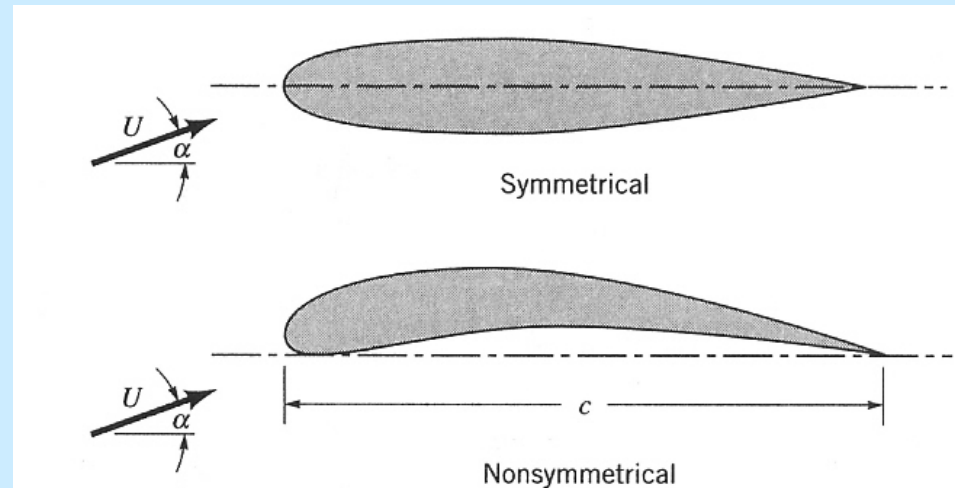


- For airfoils, the characteristic area A is the planform area in the definition of both C_L and C_D . For a rectangular planform wing, $A=bc$, where c is the chord length, b is the length of the airfoil.
- Typical $C_L \sim O(1)$, i.e., $L \sim (\rho U^2/2)A$, and the wing loading $L/A \sim (\rho U^2)/2$:
Wright Flyer: $1.5 \text{ lb} / \text{ft}^2$
Boeing 747: $150 \text{ lb} / \text{ft}^2$
- Aspect ratio $\mathcal{A} = b^2/A$ ($=b/c$ if c is constant)

In general, $\mathcal{A} \uparrow \Rightarrow C_L \uparrow, C_D \downarrow$

Large \mathcal{A} : long wing, soaring airplane, albatross, etc.

Small \mathcal{A} : short wing, highly maneuverable fighter, falcon



Lift and drag coefficient data as a function of angle of attack and aspect ratio

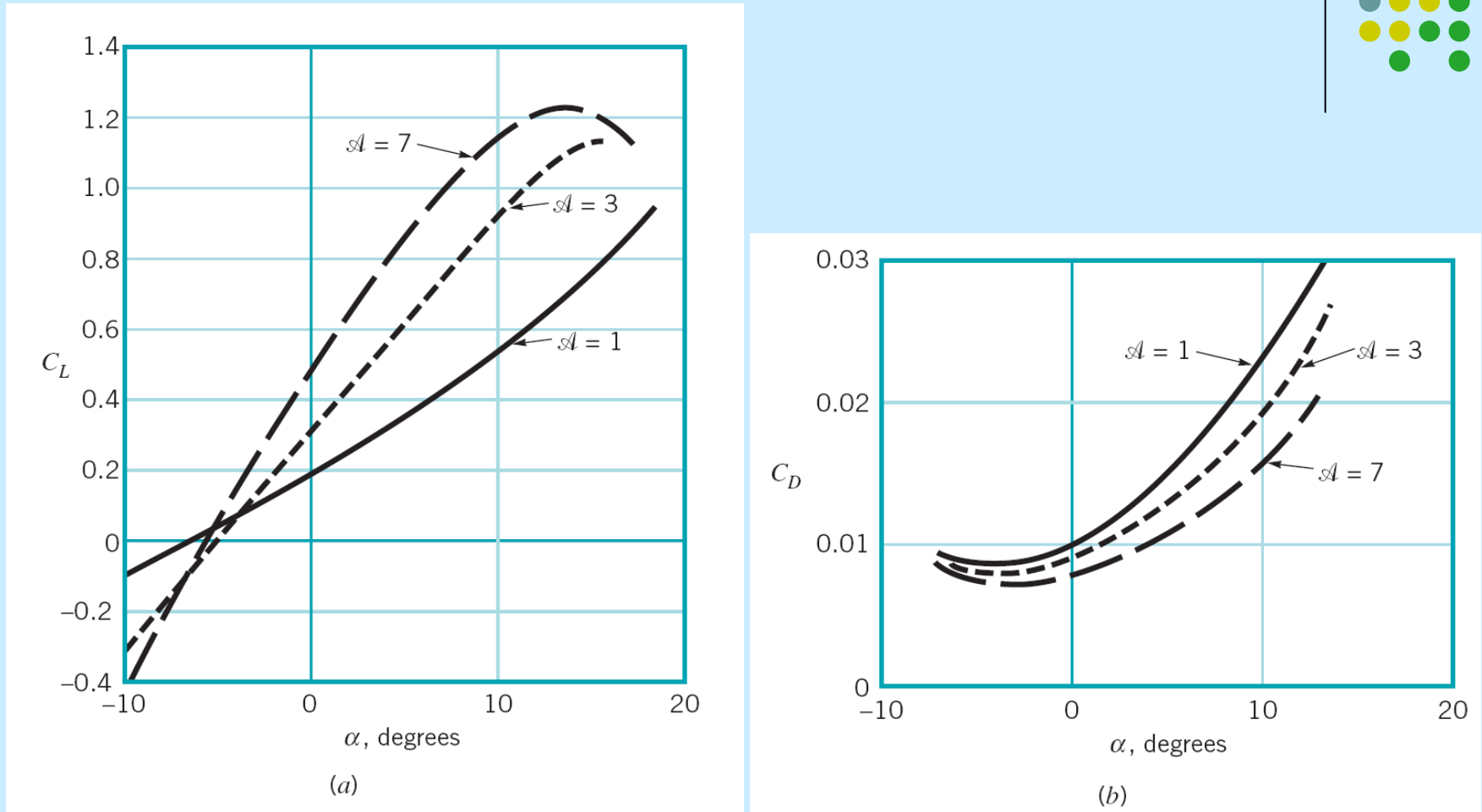
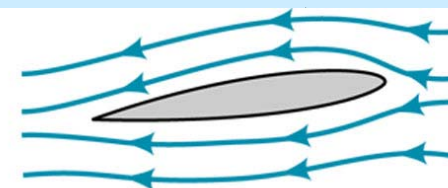
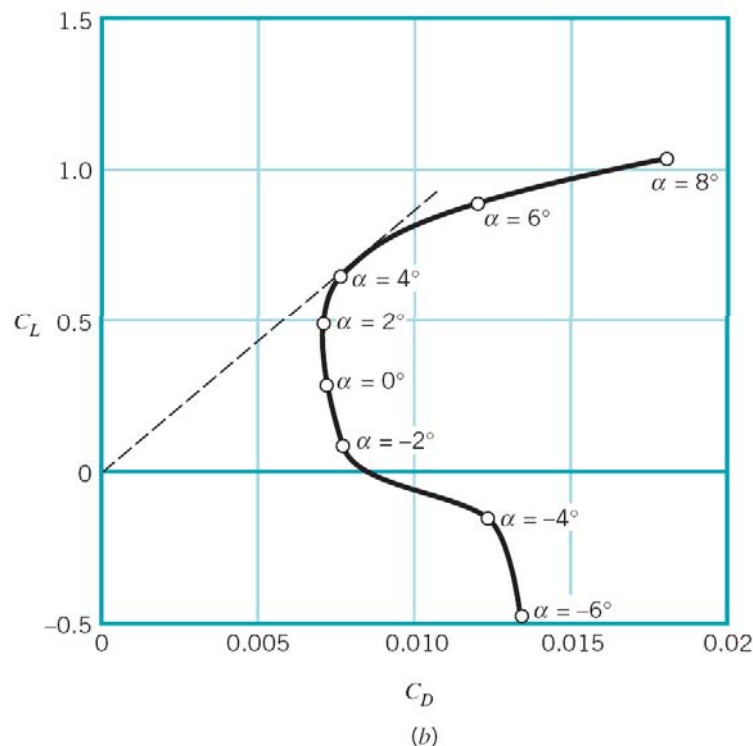
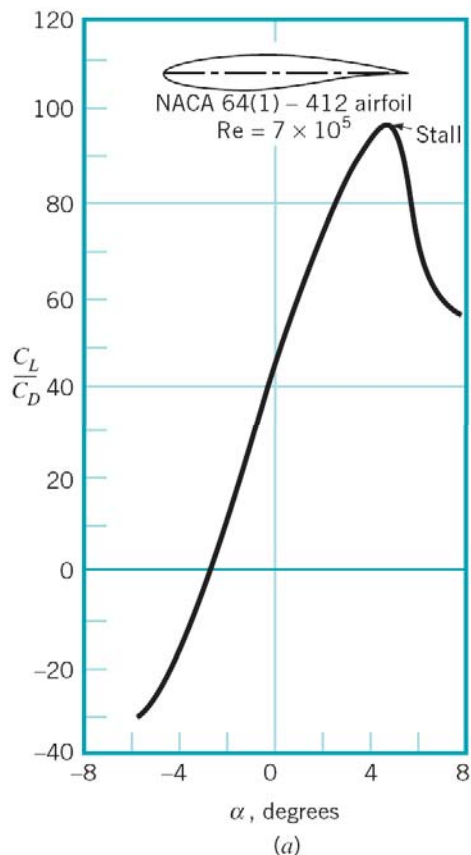


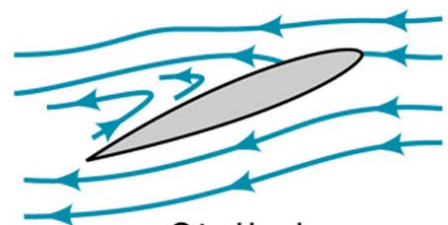
Figure 9.33

Typical lift and drag coefficient data as a function of angle of attack and the aspect ratio of the airfoil: (a) lift coefficient, (b) drag coefficient.

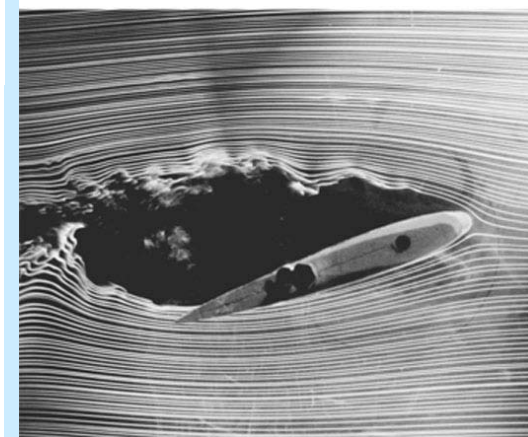
Ratio of lift to drag/Lift-drag polar



Not stalled



Stalled



V9.15 Stalled airfoil

- Although viscous effects contributes little to the direct generation of lift, **viscosity-induced boundary layer separation** can occur when α is too large to lead to **stall**.

Lift of airfoil with flap

- Lift can be increased by adding flap

V9.17 Trailing edge flap

V9.18 Leading edge flap

Ex. 9.15

Figure 9.35
Typical lift and drag alterations possible with the use of various types of flap designs (Ref. 21).

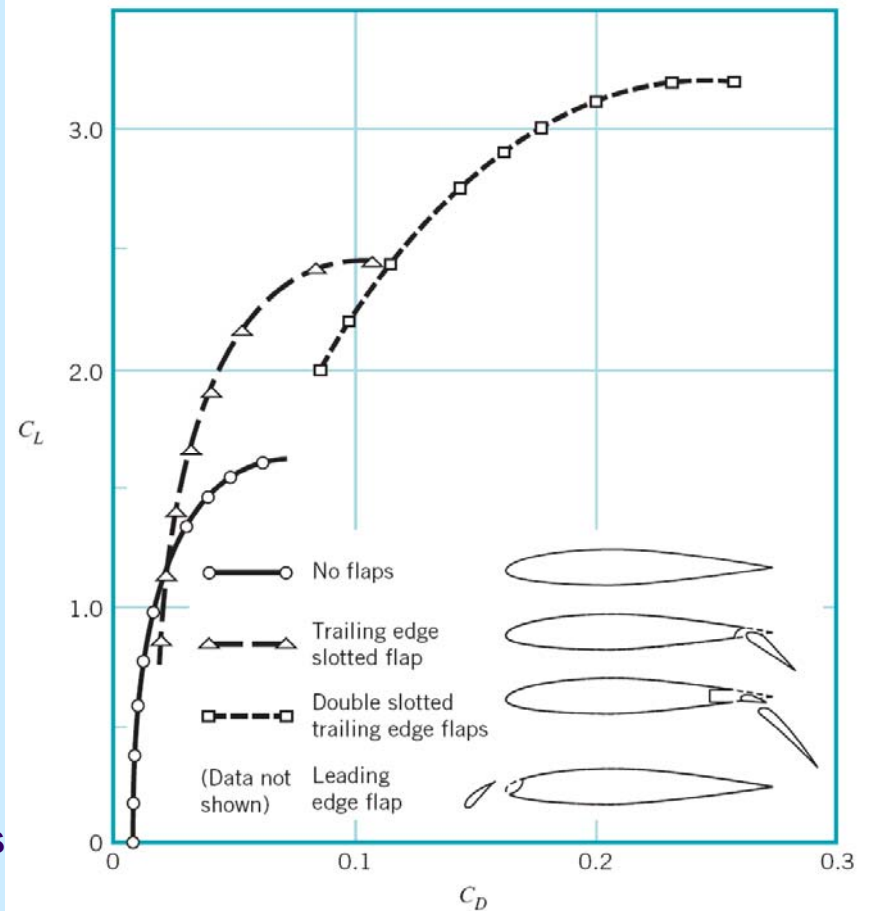


FIGURE 11-44

The lift and drag characteristics of an airfoil during takeoff and landing can be changed by changing the shape of the airfoil by the use of movable flaps.

Photo by Yunus Çengel.



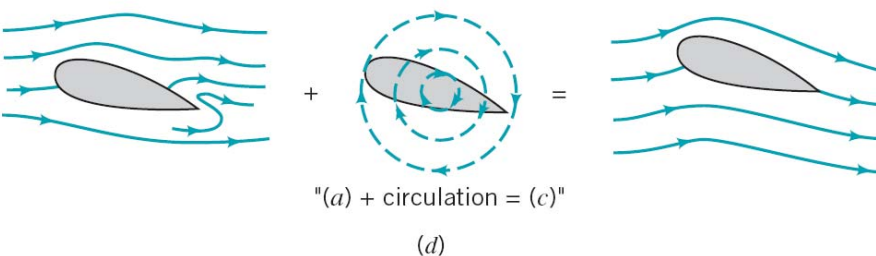
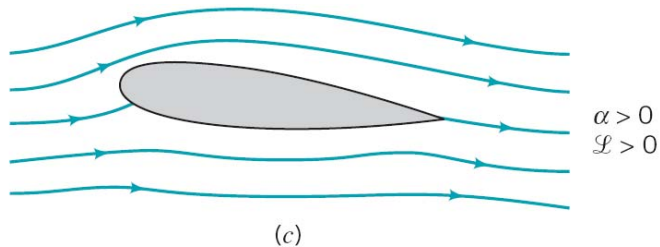
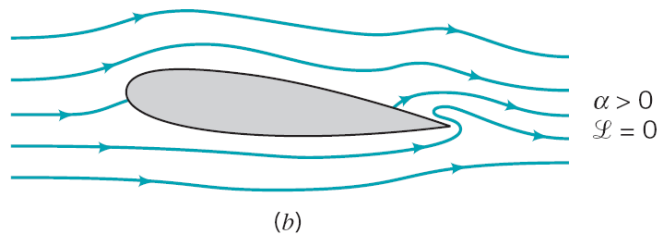
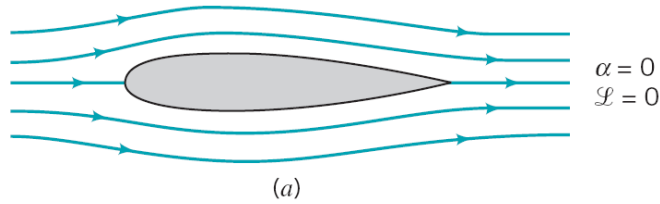
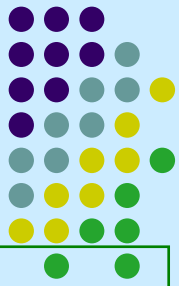
(a) Flaps extended (takeoff)



(b) Flaps retracted (cruising)

9.4.2 Circulation

2-D symmetric air foil



Kutta condition—The flow over both the topside and the underside join up at the trailing edge and leave the airfoil travelling parallel to one another.

--by inviscid theory

--adding circulation

Note: The circulation needed is a function of airfoil size and shape and can be calculated from potential flow theory.

(Section 6.6.3)

$$L = -\rho U \Gamma \quad (\text{Kutta-Joukowski Law})$$

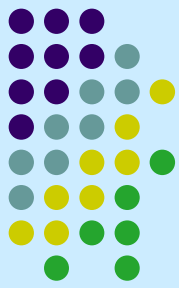
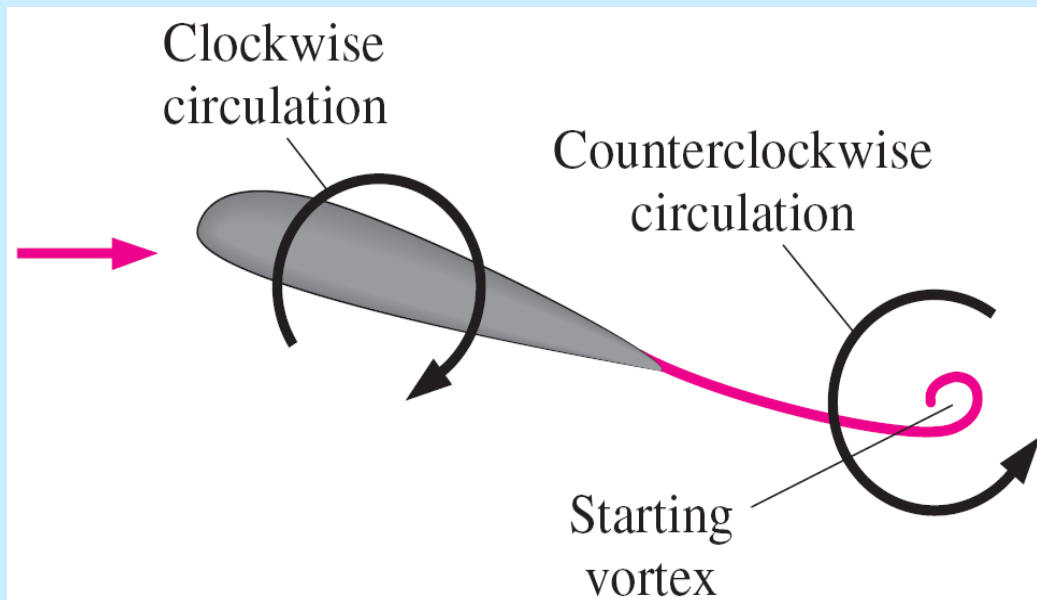


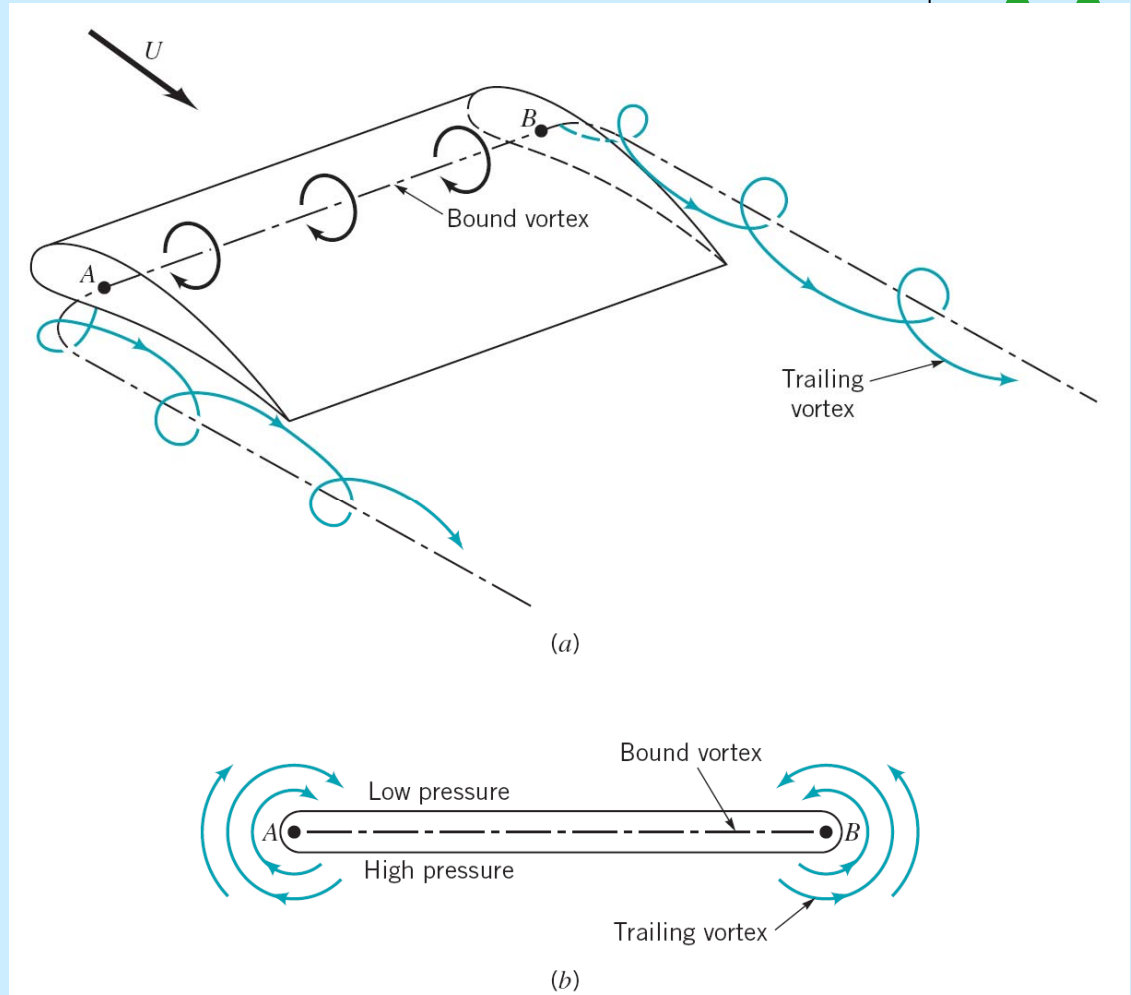
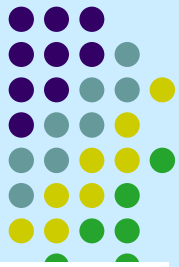
FIGURE 11-42

Shortly after a sudden increase in angle of attack, a counterclockwise starting vortex is shed from the airfoil, while clockwise circulation appears around the airfoil, causing lift to be generated.

Circulation

Flow past finite length wing

Figure 9.37 (p. 546)
Flow past a finite length wing: (a) the horseshoe vortex system produced by the bound vortex and the trailing vortices: (b) the leakage of air around the wing tips produces the trailing vortices.



V4.6 Flow past a wing

V9.19 Wing tip vortex



- Vee-formation of bird -- 25 birds fly 70% farther than 1 bird

Circulation

Flow past a circular cylinder

- A rotating cylinder in a stationary **real fluid** can produce circulation and generate a lift—**Magnus effect**

EXAMPLE 9.16 Lift on a rotating table tennis ball

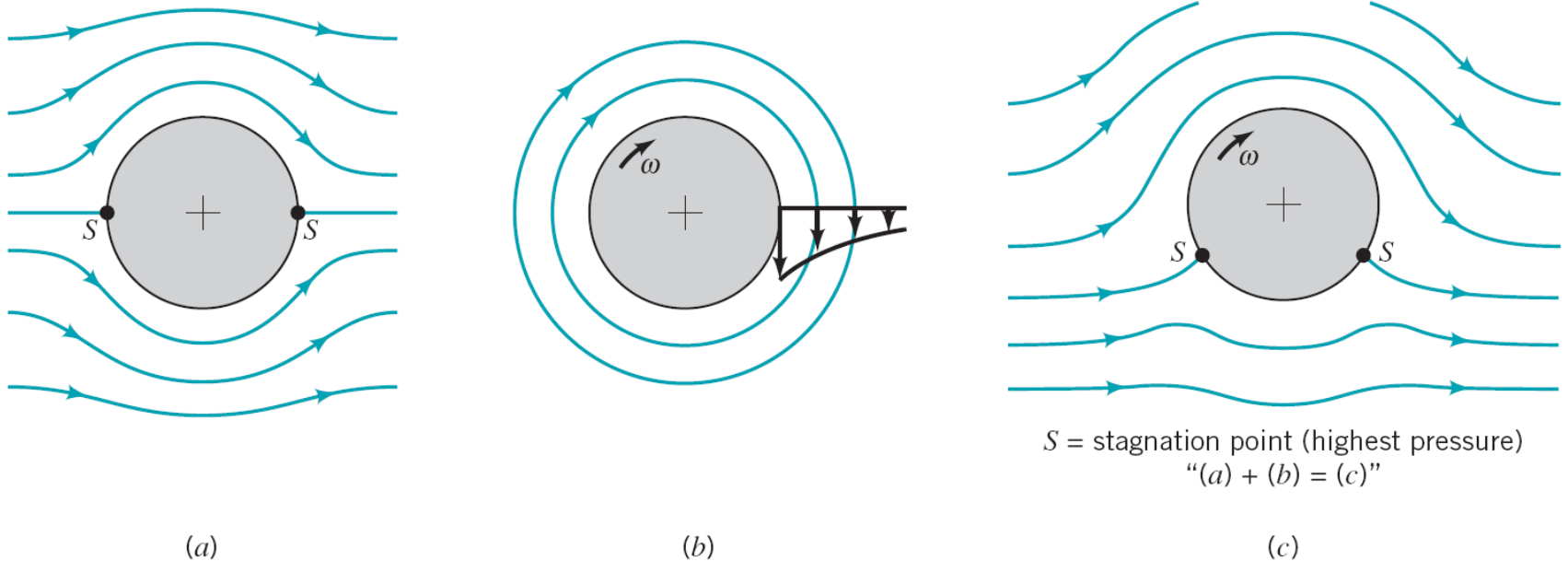


Figure 9.38

Inviscid flow past a circular cylinder: (a) uniform upstream flow without circulation. (b) free vortex at the center of the cylinder, (c) combination of free vortex and uniform flow past a circular cylinder giving nonsymmetric flow and a lift.